FACULDADE DE ENGENHARIA DA UNIVERSIDADE DO PORTO

Experimental Assessment of 4G and 5G Technologies in Varied Propagation Scenarios

Hugo Guia

FEUP FACULDADE DE ENGENHARIA UNIVERSIDADE DO PORTO

Mestrado Integrado em Engenharia Eletrotécnica e de Computadores

Supervisor: Ana Cristina Costa Aguiar

July 30, 2021

Abstract

The goal of this research project is to establish a performance comparison of two broadband cellular network technologies: Fourth Generation Long Term Evolution (4G LTE) versus Fifth Generation New Radio (5G NR). To establish the said comparison and reach precise conclusions, the impact of propagation phenomena such as path loss and shadowing on the received power and on throughput will be evaluated.

The work in this dissertation revolves around data captured in thirteen different paths surrounding the base station, which can be differentiated by its position regarding existing buildings (indoor, outdoor, mixed indoor-outdoor scenario) and the path line of sight towards the base station (line of sight, shadow non line of sight, obstructed non line of site, mixed scenario).

During the whole duration of the test, information regarding the received power and throughput is collected in a phone using specific software. The data is then processed plotting different graphics relating power, throughput and signal quality versus time and distance to reach conclusions about the performance for each scenario. Since the aforementioned information is not yet quantified, a series of propagation models are employed in order to extrapolate, based on the existing information, data for different distances in the same conditions.

With that information obtained in this work, for the same scenarios, 4G outperforms 5G with this comparison being more evident in indoor scenarios where the performance of 5G is generally poor.

Keywords: 4G, 5G, RSRP, RSRQ, throughput, path loss, modeling

Resumo

O objectivo desta dissertação é a de estabelecer uma comparação de desempenho entre duas tecnologias de redes celulares de banda larga: Fourth Generation Long Term Evolution (4G LTE) versus Fifth Generation New Radio (5G NR). Para estabelecer essa comparação e alcançar conclusões precisas, será avaliado o impacto de fenómenos de propagação como o *path loss* e o *shadowing* na potência recebida e no *throughput*.

O trabalho consiste na captura de dados em treze caminhos diferentes situados à volta da estação base que podem ser diferenciados pela sua posição relativamente aos edifícios existentes: cenário interior, exterior, cenário interior e exterior misto e a linha de visão do caminho em direcção à estação base: linha de visão, sombra sem linha de visão, sem linha de visão e obstruída, cenário misto.

Durante toda a duração do teste, a informação relativa à potência recebida e ao *throughput* é recolhida no telefone utilizando software específico. Os dados são então processados traçando diferentes gráficos relacionando potência, *throughput* e a qualidade do sinal versus tempo e distância de forma a obter informação relativa ao desempenho para cada cenário. Uma vez que a informação acima referida ainda não está quantificada, são utilizados vários modelos de propagação a fim de extrapolar, com base na informação existente, dados para diferentes distâncias para as mesmas condições.

Com a informação obtida neste trabalho, para os mesmos cenários, o desempenho da rede 4G é superior ao do 5G sendo esta comparação ainda mais evidente para cenários interiores onde o desempenho do 5G é globalmente mais fraco.

Keywords: 4G, 5G, RSRP, RSRQ, throughput, path loss, modelação

Acknowledgements

Ao longo da muralha que habitamos, pessoas houve que a meu lado me ajudaram a construir o percurso que culmina com a publicação desta dissertação.

A princípio teço uma palavra de enorme apreço à professora Ana Aguiar pela condução que fez desta dissertação aos mais variados níveis. Pelo seu apoio científico, e sobretudo pela forma como me encerebrou ferramentas e metodologias que me permitiram desenvolver o meu *magnum opus* académico acionando o máximo das minhas faculdades intelectuais; ao João Neves com quem tive a felicidade de partilhar a parte final do meu percurso académico e, principalmente, a elaboração deste projeto, pela forma como partilhamos ferramentas e entreajuda constante nas nossas dissertações.

A todos com quem me foi possível privar através das minhas responsabilidades no laboratório de redes da faculdade, entre funcionários, alunos, professores, et al, pelo espirito de constante crescimento pessoal e profissional que me dotou de capacidades para colmatar problemas e a aprendizagem persistente que me permitiu almejar para ultrapassar o impossível.

De todos os mencionados neste pequeno excerto, as palavras mais importantes e impossíveis de escrever são dirigidas a meu pai, a minha grande referência em todas as componentes pelas quais guio a minha vida e a minha forma de ser, a pessoa em quem me inspiro constantemente e almejo de forma assintótica.

Um eterno agradecimento à minha mãe por todos os valores que me incutiu e pela forma como sempre me transmitiu a responsabilidade de alcançar todos os meus objetivos sem olvidar por um instante que fosse quem me rodeia. A forma etérea com que me acompanha nos momentos mais árduos é a sua maior presença.

A toda a minha família; aos meus padrinhos que sempre estiveram presentes como segundo par parental, aos meus tios, primos, avós, pela forma como sempre me incentivaram e ergueram toda uma plataforma a permitir que os meus propósitos fossem sempre mais abrangentes. A persistência extensa pelo tempo que deles herdei permitiu que as minhas conquistas fossem sequência das suas. A eles, filhos dos homens que nunca foram meninos, lhes agradeço profundamente.

Aos primos Afonso, Gonçalo, Inês, Rita e Frederica por serem os irmãos que nunca tive.

À Mariana, por tudo, embora ela ainda não perceba e talvez nunca venha a perceber porquê.

Ao meu avô Alfredo, meu primeiro professor e educador. O Alfredo ensinou-me a ler e a contar, talvez dos instrumentos mais importantes da vida. Abriu-me horizontes infinitos e recursivos ainda hoje por explorar. Devo ao Alfredo a intensidade com que vivo a liberdade e em como não apenas sonhar com um mundo melhor, mas como agir diariamente para tornar o mundo um lugar melhor.

À minha avó Laurinda, não obstante o seu analfabetismo, a pessoa com quem mais aprendi em toda a minha vida. Dela ouvi palavras nunca escritas e pensamentos impercetíveis. O seu exemplo de persistência e resiliência é força motriz que me encoraja a ter forças para ultrapassar qualquer empecilho no caminho.

A todos os professores e educadores que se cruzaram no meu percurso académico que aqui culmina e com quem aprendi tudo, sobretudo do que não ficou por ensinar. De todos, devo endereçar

um especial agradecimento à professora Ana Traila Campos onde a pedagogia transitou para uma amizade especial e a quem devo tanto.
À Engenharia Radio, a casa dos amigos certos, em particular aos amigos Gonçalo, João, João, Jorge e Manuel que me ensinaram o valor da amizade e com quem partilhei alguns dos melhores momentos do percurso académico que agora encerra. Quase sem dar por ela, o mundo da rádio universitária transmitiu ensinamentos e valores que se tem traduzindo em mais valias nas mais diversas componentes da vida.
Para terminar este texto, não menos importantes, um muito sentido agradecimento aos amigos com quem me fui cruzando ao longo do tempo e que tanto me marcaram pela forma como sempre estiveram do meu lado nas mais adversas tormentas. Enumero, de forma associativa: Adriana, Alfredo, Beatriz, Carlos, Carolina, Catarina, Clara, Francisco, Helena, Inês, Isabel, João, Lídia, Raquel, Rita, Sofia.

Hugo Guia

"Faz-se luz pelo processo
de eliminação de sombras."

Mário Cesariny de Vasconcelos

Contents

List of Figures

List of Tables

Abbreviations

CSV	Comma Separated Value
DL	Downlink
E-UTRA	Evolved Universal Mobile Telecommunications System (UMTS) Terrestrial Radio Access
LOS	Line of Sight
LTE	Long Term Evolution
NR	New Radio
OFDM	Orthogonal Frequency Division Multiplexing
PDCP	Packet Data Convergence Protocol
RAN	Radio Access Network
RSRP	Reference Signal Received Power
RSRQ	Reference Signal Received Quality
RSSI	Received Signal Strength Indicator
UE	User Equipment

Chapter 1

Introduction

1.1 Context

The focus of all hitherto existing cellular broadband networks has been human communications. In the 5G standard the core of the system is not found in human communications or mobile Internet services. The great difference stands out in the increase of wireless device communications as sensors and embedded systems among others. In short, devices not operated directly by humans. [27]

At the present time, there has been a natural increase in the adoption of the 5G standard. Although still under development, there is already a large amount of information about what to expect [9] from it and its main focus.

Despite the existence of theoretical characterisations and pilot projects, there is yet not plenty in real-world scenarios and end-to-end communication performance, such as throughput.

As so, there is still plenty of room to improve the technology even more in order to solve issues which have already been solved in other cellular network iterations.

1.2 Motivation

Progress is heavily dependant on the constant technological evolution. Therefore, it is of the maximum interest of mankind to integrate 5G technology in the daily life of people as far as mobile communications are concerned.

Recently, a 5G base station has been installed in FEUP to be used in scientific and research projects. Due to this reason, the station in question hasn't been used after its installation and, therefore, it is of maximum interest to get to know how it operates, the features it offers and, most importantly, its behaviour in terms of signal coverage and service.

As 5G has not reached its full potential yet, there is plenty of room for a vast number of improvements in the technology, which can be reached particularly via experimental tests regarding its performance in different scenarios. One of the first steps is to characterise the performance of the radio link, and understand the propagation phenomena at 5G mid-band, at 3.5GHz, where other technologies have not been used extensively. Taking this into account, it is of great value and interest to be able to achieve groundbreaking discoveries in this area.

1.3 Objectives

The main aim of this dissertation is to perform a comparison between 4G and 5G technologies in different propagation scenarios by taking an empirical approach. The work will take advantage of a 4G/5G node B base station located in FEUP and a 5G ready smartphone.

In a first stage, a comprehensive study on the coverage and consequent quality of the 4G and 5G signals in different atmospheric and physical conditions is developed. Once these values have been collected, prepare them so that they can be analysed and reach further conclusions.

Subsequently, propagation models from the literature are fitted to the measured data to quantify the differences in order to develop a way to quantify the measurements and allow for its usage for different distances and similar scenarios.

1.4 Layout

This dissertation is structured in five chapters. Excluding this introductory chapter, the remainder are structured as follows:

- Chapter 2: Theoretical Review - This chapter provides an overview of concepts addressed in this thesis;
- Chapter 3: Proposed Approach - This chapter displays the formulation of the problem tackled in this work along with the devised strategy for the proposed solution;
- Chapter 4: Setup - This chapter consists on an explanation on how the proposed solution was accomplished;
- Chapter 5: Results - In this chapter the results achieved are further explained;
- Chapter 6: Conclusion - This chapter concludes this dissertation by presenting the main findings from this work and references future works.

Chapter 2

Theoretical Review

In this chapter concepts relevant to the development of this dissertation are presented. Firstly, characteristics related to the 5G technology, and later, an explanation regarding propagation phenomena and models as well as their intersectionality with cellular networks.

2.1 Cellular Networks

With the advent of 5G, cellular networks are now on their fifth iteration. Over thirty years, there has been a constant evolution of the technology and each generation brings with it important innovations that stand out as a way to differentiate it from its predecessors [17]. It occurred in the conversion from analogue to digital protocols between the first and second generation, the inclusion of broadband data transmission services for the third generation and the total conversion to IP services in the fourth generation [15]. As well as the aforementioned improvements in service quality, there has also been an evolution in the physical layer. [33] Initially, mobile communication resorted to TDMA, then CDMA and currently OFDMA [14]. A variation of the latter called "New Radio" is that used by the 5G standard [21]. This specification is officially named 5G non-standalone (NSA) in a way that 5G New Radio implementation is made on top of existing 4G systems [25] [33]. In this scenario, a device depends on the existing LTE infrastructure and protocols for control operation while the data can be split among 5G NR and LTE correspondent to the architecture "LTE assisted, EPC connected" [1] [11]. Figure 2.1 represents the difference between non-standalone access and standalone access.

5G breadth allows the support of different types of traffic which can be characterised as following [20]:

1. URLLC, Ultra-Reliable and Low Latency Communications, for low frequency bands, which improve in wide-area scenarios and indoor coverage;

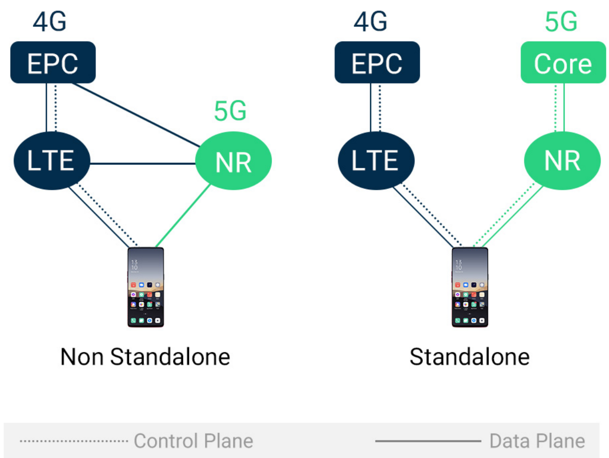

Figure 2.1: The two 5G network modes: NSA (Non-Standalone Access) and SA (Standalone Access). (adapted from [4]).

2. mMTC, Massive Machine Type Communications, for mid frequency bands in scenarios where a conciliation between performance and coverage is needed;

3. eMBB, Enhanced Mobile Broadband, taking advantage of high frequency bands for situations requiring large data rates

One of the key technologies which enables this support is Massive Input Massive Output (MIMO), an antenna technology in which for each communication various antennas are used in order to allow spatial multiplexing, and also to increase the capacity of the link to a given terminal [32] [23].

The electromagnetic spectrum ranging from 1 GHz up to 100 GHz is available for 5G. However, for the sake of maintaining backward compatibility with existing standards, it also operates in frequencies lower than 6 GHz, more precisely in the 3.5 GHz band [6]. Since higher frequency signals are more attenuated by obstacles, i.e. signals in the millimetre wave, they are not cost-effective for environments which have obstacles between the two stations to communicate, even though they allow for better transmission speeds. Therefore, for the development of this dissertation, aforementioned frequencies will be ignored [26]. In Figure 2.3 the frequency bands for all cellular network technologies are shown. For 5G there is a plethora of frequency bands available which change for each country due to spectrum availability. For Europe, Figure 2.4 presents that the focus has been on mid-band frequencies (3.4-3.8 GHz) and high-band frequencies (26-27.5 GHz).

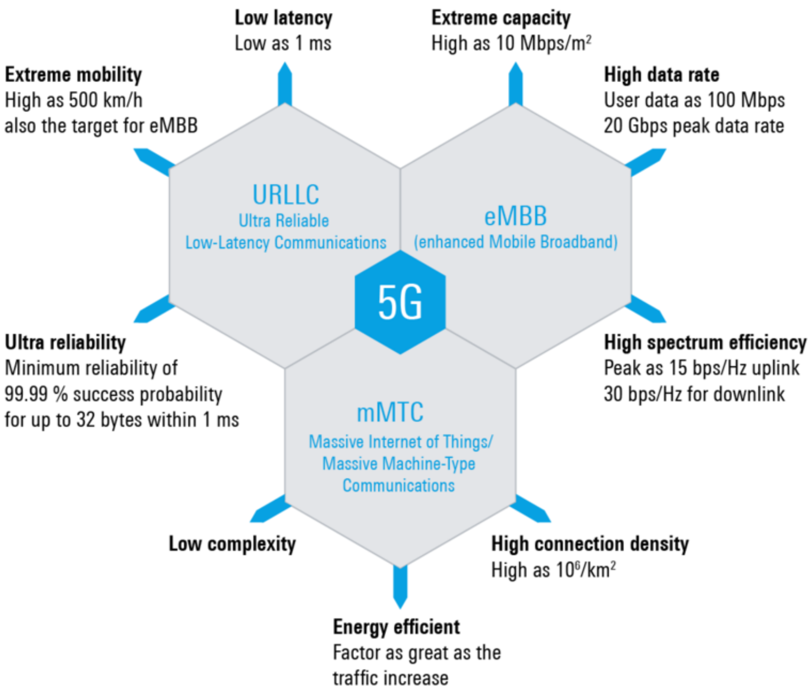

Figure 2.2: Objectives of 5G according to the International Telecommunication Union (adapted from [20]).

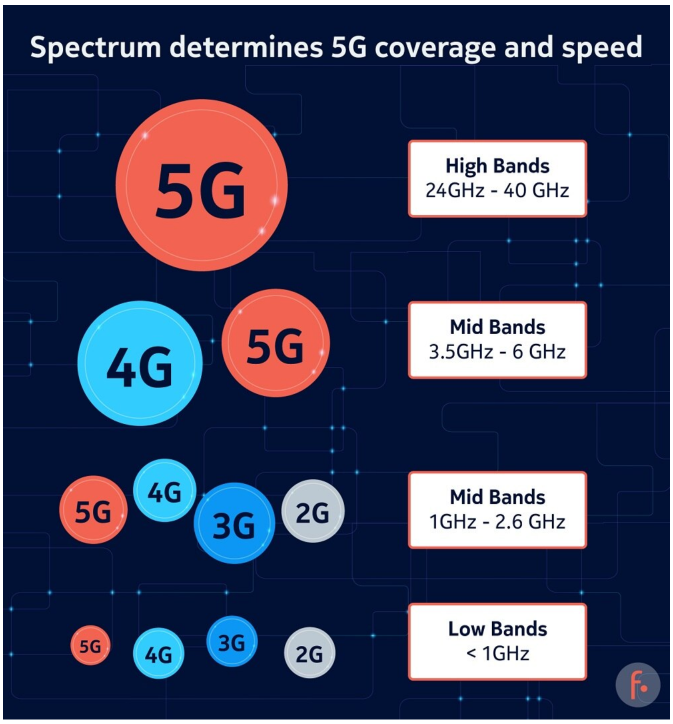

Figure 2.3: Spectrum used by each of the different cellular technologies (adapted from [5]).

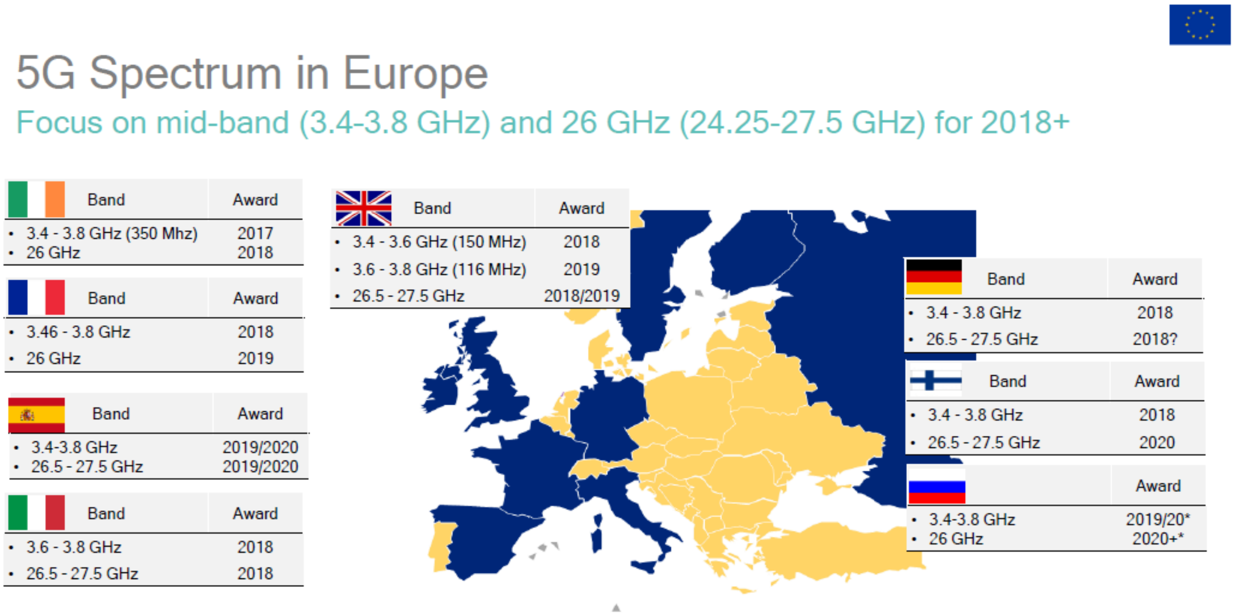

Figure 2.4: 5G spectrum in Europe (adapted from [2]).

One aspect of New Radio physical layer that affects greatly 5G performance is the concept of beamforming. Although not being a new conception as current LTE networks resort to it, the challenges brought by 5G regarding signal propagation issues encourage its broader usage. For frequencies above 24 GHz, the usage of analog beamforming of narrower beam widths grants the possibility for 5G base stations to more precisely be able to steer downlink signals. The process consists in beam scanning in order for the base station to identify the most accurate beam location regarding a specific mobile device. The usage of this approach allows for the smartphone's downlink transmission to benefit from higher signal strength, specially due to using modulation schemes of higher order. Nonetheless, beamforming also introduces several challenges. Not only does each beam need to be defined and tested, but also over-the-air measurements are crucial to validate radio performance [12].

2.2 Propagation phenomena

In the electromagnetic spectrum, the electromagnetic wave propagation is affected by several phenomena that reflect themselves as channel attenuation. Channel impediments such as noise, interference and others tend to vary in time and in unpredictably ways dependending on the movement of the user. In this chapter, the variation of the received signal strength due to free space path loss and shadowing will be characterised. The first is characterised by the dissipation of radiated power by the transmitter as well as channel propagation effects, while the latter is characterised by the existence of obstacles between the transmitter and the receiver which absorb radiated power. When full absorption occurs, the signal is blocked. Variations due to path loss are more dominant for higher distances (in the range of 100-1000 metres) [29] while variations relative to shadowing are more prominent at distances proportional to the length of the obstruction (10-100 metres outside, less inside). As these variations occur over wide distances, they are commonly referred to as local mean attenuation or large-scale propagation effects. [16]

Electromagnetic waves spread through various environments in which they are reflected, refracted, scattered and diffracted on walls, buildings and other objects. Although Maxwell's equations can be used to obtain details concerning the propagation of these waves, they are complex and not all situations guarantee the availability of all parameters for this calculation. Therefore, approximations are developed in order to characterise the propagation of the signal without having to resort to those equations.

The most common approaches make use of ray tracing techniques. These are characterised by a representation of the wavefront as a simple particle, i.e. it determines reflection and refraction on the wavefront but ignores more complex dispersion. The model with the highest degree of simplicity is known as two-ray model, which summarises the propagation of the signal between a transmitter and a receiver as a direct path and one reflected path. The reflected path usually bounces on the ground. This model ensures a good approximation of propagation for motorway, rural and water-based scenarios. Since many propagation environments are not effectively portrayed by ray tracing models, the development of analytical models based on empirical measures is necessary in some circumstances. [16]

2.3 Propagation models

The complexity of signal propagation makes it difficult to obtain a unique model which characterises path loss as accurate among a vast amount of distinct environments. These models of path loss measurement can be obtained either via complex deterministic models of ray tracing or through empirical evaluation where system specifications need to be established or to determine the best location for base stations and access points. In general, as far as system design analysis goes, it's more prudent to apply simple models which relate as an approximation of the real channel. An example is the the free space path loss. Considering a scenario where a signal sent by a transmitter to a receiver located at a distance *d (m)* and assuming that there are no obstructions between them and that the signal propagates along a straight line between them. The channel model associated with the transmission is described as line-of-sight channel and the corresponding received signal from LOS signal or ray. The received signal can be expressed as follows: [16]

$$r(t) = R\left\{ \frac{\lambda \sqrt{Gl} e^{-j\left(\frac{2\pi d}{\lambda}\right)}}{4\pi d} u(t)\, e^{j2\pi fct} \right\}; \tag{2.1}$$

Being Pt the power of the transmitted signal s(t), the ratio between received and transmitted power can be calculated as: [16]

$$\frac{Pr}{Pt} = \left[\frac{\sqrt{Gl}\lambda}{4\pi d} \right]^2 \tag{2.2}$$

Therefore, one can conclude that, for free space path loss, the power of the received signal is inversely proportional to the square root of the distance d between transmission and reception antennas. The free space path loss is defined as path loss of a free space model as: [16]

$$P_L\,[dB] = 10\log_{10}\left(\frac{Pt}{Pr}\right) = -10\log_{10}\left(\frac{Gl\lambda^2}{(4\pi d)^2}\right) \tag{2.3}$$

A more simplified version of this model for path loss calculation as a function of distance is shown here: [16]

$$Pr = PtK\left[\frac{d_0}{d}\right]^{\gamma} \tag{2.4}$$

The dB attenuation is as follow:

$$Pr(dBm) = Pt(dBm) + K(dB) - 10\gamma\log_{10}\left(\frac{d}{d_0}\right) \tag{2.5}$$

2.3.1 Empirical path loss models

The majority of mobile communication systems work in propagation environments so complex that they cannot be precisely detailed via free-space path loss, ray tracing or simplified models. Due to that reason, a large number of models are being developed through the years in order to predict the aforementioned path loss in typical wireless communication scenarios such as macro and micro urban cells and, more recently, inside buildings. These models are predominantly based on empirical evaluations relative to specific distances, frequency ranges and geographical areas. However, since the usage of said models is not strictly dependent on the scenarios for which they were developed, these can be used favourably in other scenarios.

2.3.2 Okumura model

One of those models of signal prediction in urban environments is the Okumura's model. It is used in distances ranging from 1 to 100 km and frequencies ranging from 150 to 1500 MHz. The formula to measure the path loss is as follow [16]:

$$L_{50}\,(dB) = L_f + A_{mu}(f, d) - G(h_t) - G(h_r) - G_{area} \tag{2.6}$$

2.3.3 Walfisch/Bertoni model

Proposed by Walfisch and Bertoni, this model acknowledges the effect of rooftops and buildings in diffraction suffered by the signal. According to this model, path loss can be measured by the product of [16]:

$$L = P_0 Q^2 P_1 \tag{2.7}$$

Where P_0 is the free space path loss for omnidirectional antennas, Q^2 considers the signal power reduction due to blockages by buildings at street level and P_1 is the signal loss from the rooftop to the street due to the effect of diffraction.

2.3.4 Alpha Beta Gamma model

The Alpha Beta Gamma (ABG) model encompasses a generic all-frequency model for large-scale propagation path loss in pertinent frequencies from the mid-band frequency range spawning from 1 to 6 GHz [28]. Its equation is as follow:

$$PL^{ABG}(f,d)[dB] = 10\alpha \log_{10}\left(\frac{d}{1m}\right) + \beta + 10\gamma \log_{10}\left(\frac{f}{1GHz}\right) + \chi^{ABG} \tag{2.8}$$

2.3.5 Close In model

This model is similar to Alpha-Beta-Gamma in its implementation except it only has one parameter to be optimised. It is based on the Free Space Equation which considers the wavelength of the propagated signal, therefore, the physical anchoring of the model is represented by the FSPL [22].

$$PL^{CI}(f,d)[dB] = FSPL(f,1m)[dB] + 10n\log_{10} d + \chi^{CI} \tag{2.9}$$

$$FSPL(f,1m)[dB] = 20\log_{10}\left(\frac{4\pi f}{c}\right) \tag{2.10}$$

2.4 UE measurement capabilities

In this section, some UE measurement quantities are explained.

2.4.1 LTE

2.4.1.1 RSSI

E-UTRA Received Signal Strength Indicator (RSSI), encompasses the linear average of the total received power (in [W]) observed specifically in the configured OFDM symbol and in the measurement bandwidth over N number of resource blocks, by the UE from all sources, including co-channel serving and non-serving cells, adjacent channel interference, etc. On higher layers, the duration of the measurement and which OFDM symbol(s) to be measured by the UE can be found. The antenna connector of the UE shall be the reference point for the RSSI. In case of receiver diversity by the UE, the reported value shall not be lesser than the corresponding RSSI of any of the individual branches [10].

2.4.1.2 RSRP

Reference signal received power (RSRP), is characterised as the linear average over the power contributions (in [W]) of the resource elements that transport cell-specific reference signals contained within the considered measurement frequency bandwidth. In order to determine RSRP, the cell distinct reference signals on antenna port 0 are used, with the UE using port 1 in case it is also detected. In the scenario where higher layers reveal measurements based on discovery signals, RSRP in the subframes is also measured by the UE. The antenna connector of the UE serves as the reference point for the RSRP. In the case of receiver diversity in use by the UE, the reported value must not be lesser than the corresponding RSRP of any of the individual diversity branches [10].

2.4.1.3 RSRQ

Reference Signal Received Quality (RSRQ) is described as the ratio NxRSRP/(E-UTRA carrier RSSI), where N is the number of RB's of the E-UTRA carrier RSSI measurement bandwidth. The same set of resource blocks shall be used in the measurements. If higher layers indicate all OFDM symbols for performing RSRQ measurements, then RSSI is measured from all OFDM symbols of the DL part of measurement subframes. The reference point for the RSRQ is expected to be the antenna connector of the UE. If receiver diversity is used by the UE, the value shall not be lesser than the corresponding RSRQ of any of the individual diversity branches [10].

2.4.2 NR

2.4.2.1 NR carrier RSSI

NR carrier Received Signal Strength Indicator (NR carrier RSSI) englobes the linear average of the total received power (in [W]) observed only in certain OFDM symbols of measurement time resource(s), in the measurement bandwidth, over N number of resource blocks from all sources, including co-channel serving and non-serving cells, adjacent channel interference, etc. For intra-frequency measurements, NR Carrier RSSI is calculated with timing reference corresponding to the serving cell in the frequency layer. For inter-frequency measurements, the measurement is made via timing reference corresponding to any cell in the target frequency layer. Otherwise, if measurement gap is not resorted to, NR Carrier RSSI is measured from OFDM symbols within SMTC window duration and, if measurement gap is used, NR Carrier RSSI is measured from OFDM symbols corresponding to overlapped time span between SMTC window duration and minimum measurement time within the measurement gap [3].

2.4.2.2 SS-RSRP

Secondary synchronisation reference signal received power (SS-RSRP) is characterised as the linear average over the power contributions (in [W]) of the resource elements that carry secondary synchronisation signals (SS). The measurement time resource(s) for SS-RSRP are confined within the duration of SS/PBCH Block Measurement Time Configuration (SMTC) window. For frequency range 1, the reference point for the SS-RSRP shall be the antenna connector of the UE. For frequency range 2, SS-RSRP shall be measured based on the combined signal from antenna elements corresponding to a given receiver branch. For frequency range 1 and 2, if there is diversity in the receiver in use by the UE, the reported SS-RSRP value shall not be lesser than the corresponding SS-RSRP of any of the individual receiver branches [3].

2.4.2.3 SS-RSRQ

Secondary synchronisation signal reference signal received quality (SS-RSRQ) is defined as the ratio of NxSS-RSRP / NR carrier RSSI, where N is the number of resource blocks in the NR carrier RSSI measurement bandwidth. The same set of resource blocks needs to be used in the measurements. For frequency range 1, the reference point for the SS-RSRQ shall be the antenna connector of the UE. For frequency range 2, NR Carrier RSSI shall be measured based on the combined signal from antenna elements corresponding to a given receiver branch, where the combining for NR Carrier RSSI shall be the same as the one used for SS-RSRP measurements. For frequency range 1 and 2, in the case that receiver diversity is in use by the UE, the reported SS-RSRQ value shall not be lower than the corresponding SS-RSRQ of any of the individual receiver branches [3].

Chapter 3

Proposed Approach and Setup

In this chapter, the problem that this dissertation revolves around is formulated and the proposed solution is detailed. Posterior to that, the setup will be further explained.

3.1 Problem Formulation

When applied in a real scenario, the performance of 4G and 5G technologies differ from one another. The problem in this work consists of evaluating the impact that specific propagation phenomena such as path loss and shadowing have on these broadband cellular network technologies at the RAN domain.

In this work, we will contrast how the signal propagates and reacts to previously mentioned phenomena in various scenarios which include line of sight scenarios and non line of sight scenarios with impediments such as shadowing, obstructions and mixed. In addition, the scenarios can also be compared relatively to their location regarding buildings, this being as either indoor or outdoor.

3.2 Proposed Approach

The first step is dedicated to making a geographical survey around the base station in order to precisely define the areas in which the tests will be conducted. After that, it is crucial to correctly categorise each path with regard to those requirements.

Afterwards, the following step is to perform a set of measurements by taking a stroll in the pre-established paths using a smartphone to perform the evaluation and to store all the information related to GPS location, time, RSRP, RSRQ and throughput.

With the previous information properly stored on the smartphone, the ensuing step is to proceed to the extraction of the gleaned information and relate them with one another in a way that allows for conclusions to be reached on an qualitative way. This can be achieved by a series of graphical plots relating:

- distance with RSRP;

- distance with RSRQ;
- distance with throughput;
- time with RSRP;
- time with RSRQ;
- time with throughput;
- RSRP with throughput;
- RSRQ with throughput;

The latter stage of this work consists in using the above-mentioned results and estimate parameters of models for the mid band in order to quantify the obtained results and use these values in a series of propagation models in order to predict the behaviour of the signal for larger distances in similar atmospheric situations and scenarios.

3.3 Geographical survey

The fact that we knew *a priori* the location of the base station within the university area allowed to more precisely better restrain the choice for the best 4G and 5G coverage in the specified area. Once the geographical research around the college *campus* was done, fourteen different paths spanning an area of approximately 0.21 km^2 were established as seen in Figure 3.1.

The foregoing paths were chosen as a result of encompassing areas which contain buildings and foliage whose hindrance on propagation is relevant for this study. These paths were then parameterized according to performance parameters mentioned in the previous chapter as it can be seen in Table 3.1:

Path	Location	Line of Sight	Within main lobe
A	Outdoor	Yes	No
B	Outdoor	Mixed	Mixed
C	Outdoor	Mixed	Mixed
D	Indoor	No	Yes
E	Indoor	No	Mixed
F	Outdoor	No	Mixed
G	Indoor	No	Yes
H	Outdoor	Yes	Yes

Table 3.1: Paths characterisation.

Paths D and G are located in the faculty main building whereas path E is located in the department of chemical engineering. Paths D and G encompass sub paths which correspond to the four levels of the building and measurements were conducted for each floor. On the other hand, even though path E only comprises of a unique measurement, this is made in multiple floors.

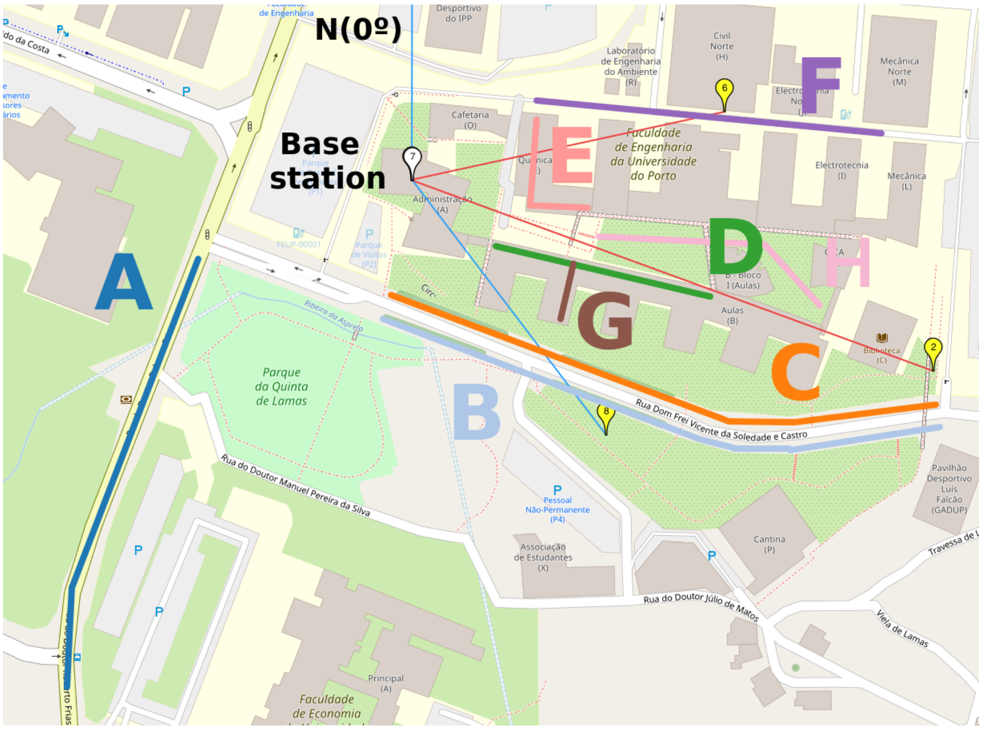

Figure 3.1: Pre-established paths where measurements were conducted in base station main lobe

3.4 Performance metrics

One important procedure is to identify what are the relevant metrics which are interesting in collecting for this specific work. Regarding UE-related measurement, the choices were between RSRP, RSRQ and RSSI. In light of the information found in section 2.4, RSRP was used as the main metric due to the information it comprises and which can be used for the modeling part of this work. Due to its qualitative value, RSRQ information will also be used in order to help to understand the RSRP data in the cases where it can be difficult to interpret the data. One metric which is also extremely relevant is the throughput. It is significant as a way to measure the amount of information transmitted in a specified time interval. The throughput value can be measured in different layers which are, in crescent order, RPS, RLC, MAC and PHY layer [7]. Due to headers and HARQ retransmission in higher layers, more information not relevant for the measurements is transmitted. So, for this work, the value of PDCP throughput located in the RPS layer is used.

3.5 Measurement methodology

The subsequent step to encountering the best path was to determine the way data was going to be gathered and how to process it.

As planned, the chosen equipment for the measurements was a 5G ready smartphone. The equipment at stake constitutes of a Xiaomi Mi 10 running Android 10 with a Qualcomm SM8250 Snapdragon 865 5G chipset. In order to extract relevant information regarding the metrics we had

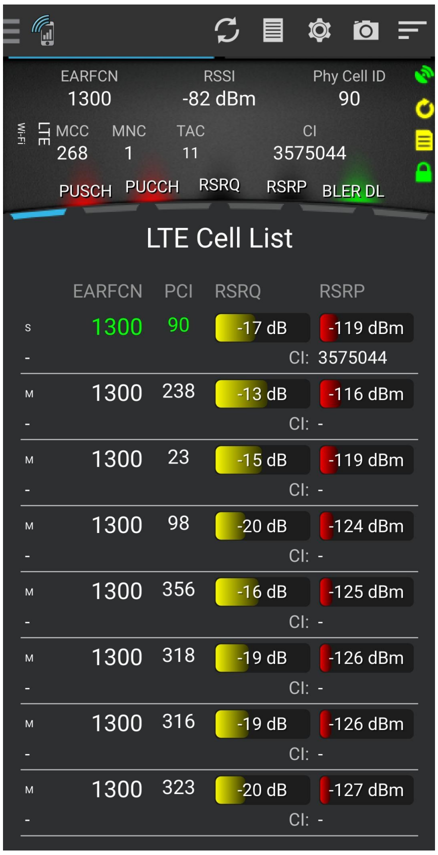

Figure 3.2: Infovista's TEMS Pocket main screen

to process, a specific software was needed for the data gathering procedure. The software, which was developed by Infovista, comprises of a multi-platform suite both for Android and Windows operating systems named TEMS. On Android, the version of the software used is called TEMS Pocket. A screenshot of the interface of the software can be seen in Figure 3.2. This software grants the possibility to lock the smartphone radio access technology to force either a 4G or a 5G connection to be established.

The software measures different metrics even though only a selected few were relevant for this study. The way this data capture is made is via its interface where a logfile in .TRP format, a binary file developed by Infovista, is generated. Each second, information is stored in this file which is stored on the smartphone. The file contains every information the software is capable of collecting. As a result, the output file can thrive to several hundreds of megabytes. From this file, the relevant information which allows for data processing and graphical plotting, as can be seen in subsequent chapters of this work, can be extracted using TEMS Investigation, on a Windows system. The way this works is by importing the .TRP file into the program which shows different information regarding the data capture. Considering the fact that only information regarding time, geographical position. RSRP, RSRQ, PDCP DL and throughput were necessary, yet another tool from the same suite was used, TEMS Export, which allows the export of the preceding information to a file in .FMT format which is no more than a CSV file. For that reason, it was more straightforward to

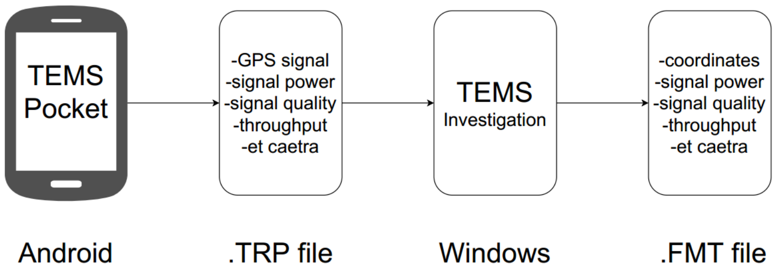

Figure 3.3: Steps to acquire data in a text file.

handle the data. The way the data was handled will be further understood in the next section.

Regarding the test, it consisted of a walk through all its length in both directions so that the test starts and ends at the same place, with exception of path E which is one way only. During these walks, the smartphone was held in hand, in front and at breast height at the speed of a stroll. In order to generate network traffic, a file was being downloaded through the whole duration of the test. The file used for the tests was a version of the operating system CentOS [1] whose server location is in the city of Porto and managed by University of Porto. The specified file was chosen for its large size and its location which allowed for a steady and long lasting connection while the test was running. The download of the file, using the smartphone's browser, was initiated before starting the data capture process in order to guarantee that there was an active connection for every coordinate of the path.

The whole process is represented in Figure 3.4.

3.6 Data assessment

The next step posterior to the gathering was to understand what to do with the data in the exported file. A series of graphical plots were planned relating the signal power vs distance, signal power vs time, signal quality vs distance, signal quality vs time, throughput vs distance, throughput vs time, throughput vs signal power and throughput vs signal quality. The priority was to relate the aforementioned elements in a graphical way and discriminate them by the set of scenarios previously defined in order to reach further conclusions.

A set of *Python* scripts were developed for that purpose in order to obtain the previously mentioned graphical plots. Tools such as matplotlib [19], numpy [18], pandas [24] and math [31] were used. Common to all scripts was the way that empty values were ignored. Considering only the valuable information needed for the plots, rows with empty latitude and longitude values were ignored, so did the ones with simultaneous empty RSRP, RSRQ and PDCP DL throughput values.

[1] http://mirrors.up.pt/pub/centos/8.3.2011/isos/x86_64/CentOS-8.3.2011-x86_64-dvd1.iso

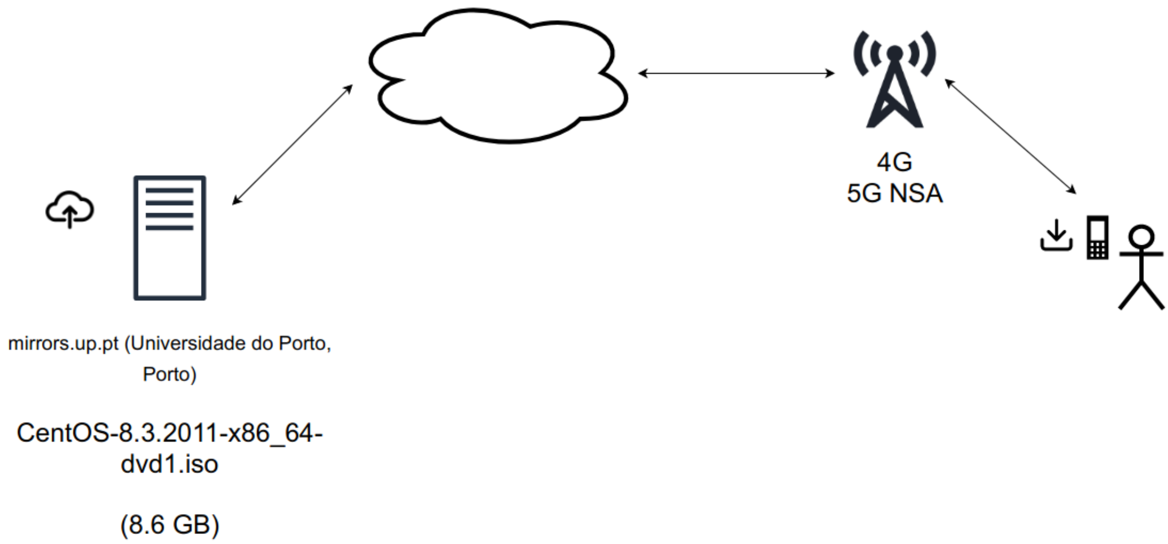

Figure 3.4: Measurement process.

3.7 Challenges in the process

The complexities inherent to this work assured beforehand that a large number of constraints would appear as the experiments were being unfolded.

The first major incident revolved around the process of installing the TEMS suite on the smartphones, known by the developers as the "TEMSification process". Due to the intricacies of the software, the process of installation is not as straightforward as other smartphone apps. As it alters the mobile technology the smartphone is using, higher permission levels within the operating system are needed. Even though the process of rooting the smartphone allows for some level of autonomy, it is not sufficient for the requested features. Therefore, a special build of the operating system with a different kernel was needed. The two smartphones initially used for this work were a Samsung S10 5G and a Xiaomi Mi Mix 3 5G. When TEMS Pocket was firstly installed, a problem revolving around not having root permissions arose. Using the open-source tool Magisk [2], the problem was quickly fixed. However, despite being able to install the software, the problems with the software persisted: we were not able to get the information desired. After further contacts with Infovista we were informed that we needed a custom version of the Android operating system for each device, as explained previously. With this information in mind, and using the required files provided by Infovista, we were successful in properly installing the software. With the software accordingly working, we were able to conduct test experiments in order to understand the tool slightly better. After experimental measurements in 4G, problems began when experimenting with 5G. The Samsung smartphone would not establish a 5G connection with the desired base station, nor any kind of 5G connectivity. This was later understood due to the fact that the 5G base station, being a test station, is not compatible with all the 5G devices available on the market which will not establish a connection. The Xiaomi smarthphone, due to an overnight

[2] https://github.com/topjohnwu/Magisk

operating system update, installed a new version of MIUI which disabled 5G connectivity. These different situations on both smartphones posed a barrier to the development of this work as 5G technology was not present and the focus of this work requires both 4G and 5G to establish the aforementioned comparison.

Following this situation, the partner operator provided us with two Xiaomi Mi 10 smartphones whose TEMSification process had already been done and we were granted that the 5G connectivity was functional in those equipment. Albeit being able to establish 5G connectivity, a new problem ensued: the GPS signal, despite working perfectly in other apps on the smartphone, seemed to have some problems with TEMS Pocket. This posed a problem as one of the key components in this process was the need to have the georeferenced position each second. After contacts with the operator and Infovista, the problem was solved by changing several application settings regarding battery management which would limit the full potential of the software. Indirectly, this could have also solved some problems that could have arisen in the future regarding the software.

At this point, after some months of constant research about functional equipment and ways to solve the prior problems, we were allowed to conduct the relevant measurements. The ensuing difficulties arose during the process of handling the data. In the first place, the most significant one was concerned to the erroneous data received in relevance to the indoor paths. The fact that the tests were conducted inside a building resulted in the GPS data being inaccurate as could be interpreted in the georeferenced plots where indoor paths were shown as being outdoor. This situation could be solved using a TEMS Pocket functionality which allowed for indoor scenarios planning and measuring the required information in specific pre determined points. [13]

Later, a different problem from the previous one yet in the same field was connected with throughput measurement. All hitherto data was measured each instant besides some time periods when the data was not available. For each instant, the information regarding position, RSRP and RSRQ was known, which allowed for direct comparison among these parameters. However, the situation regarding the throughput values was slightly different. Information regarding the throughput and both RSRP and RSRQ was exclusive, for each instant of time where the throughput value was given, the other two values were empty. This posed an issue: there was no way to directly correlate the parameters. Not being able to understand the way the values were presented, contacts with Infovista were made which informed that the way that throughput was calculated in TEMS was in compliance with the 3GPP standard regarding this topic [8].

Chapter 4

Results

In this chapter, information related to the achieved results well be displayed. It will be divided into two sections. The qualitative evaluation first, where the measured data is checked in order to reach further conclusions regarding the results. In the next section, with the data analysed in the first section, that information is applied in different propagation models.

4.1 Qualitative evaluation

4.1.1 Outdoor scenarios

The paths which consist of outdoor scenarios are five: A,B, C, F and H as seen in Figure 4.1. Furthermore, path A and H have LOS towards the base station for its whole extension, path B and C, parallel to each other as two opposite sidewalks, only get LOS in the beginning of the course whereas in the rest of the course the effect of shadowing is easily perceptible. The last in this set is path F which is NLOS for the whole path.

Overall, by direct comparison between 4G and 5G regarding RSRP versus distance as seen in Figure 4.2, one can interpret that the values are more scattered in 5G than in 4G for the same scenario. For the same distance value, the amplitude of RSRP value variation in 4G is relatively low, whereas in 5G the minimum measured value is acutely lower compared to its counterpart.

Relatively to path A, despite the fact that it has direct LOS towards the base station, it is well visible that, for shorter distances, the equivalent value of the RSRP in path B and C is higher. This can be explained taking into account the antenna orientation specially regarding the main lobe azimuth and its beam width. Path A, for the referred distances, is located outside the antenna main lobe. Therefore, only for distances higher than approximately 150m, the RSRP value is higher than its counterparts.

Path B and C values differ slightly from one another due to their close geographical position. The main difference is the foliage present which is denser for path C as vegetation, specially trees, from both sidewalks behave as an obstacle for the signal propagation.

Path F is undoubtedly the one where both 4G and 5G have the worse performance of all the outdoor scenarios. The latter does not have, throughout its entire course, any kind of line of sight towards to the base station due to being blocked by a concrete building. Not only that, but it is also contained within a canyon.

Path H is the other one which consists of a LOS scenario. However, and contrarily to path A, it is completely located within the antenna's main lobe. This complies to the aforementioned explanation regarding low RSRP in path A for shorter distances.

By observing the RSRP versus throughput plots in Figure 4.4 one can assess that instances correlating both metrics simultaneously are more abundant for 4G. For path A in particular, for the same RSRP values, the throughput value is superior in 5G and there are less instances of low throughput in comparison with 4G. This is due to the fact that 5G compensates the losses by sending increased data bursts each iteration [30]. One relevant aspect is related to path H which, despite having a consistent performance in 4G throughout its length, has the lowest RSRP and throughput of all the outdoor paths for 5G with the poorest performance.

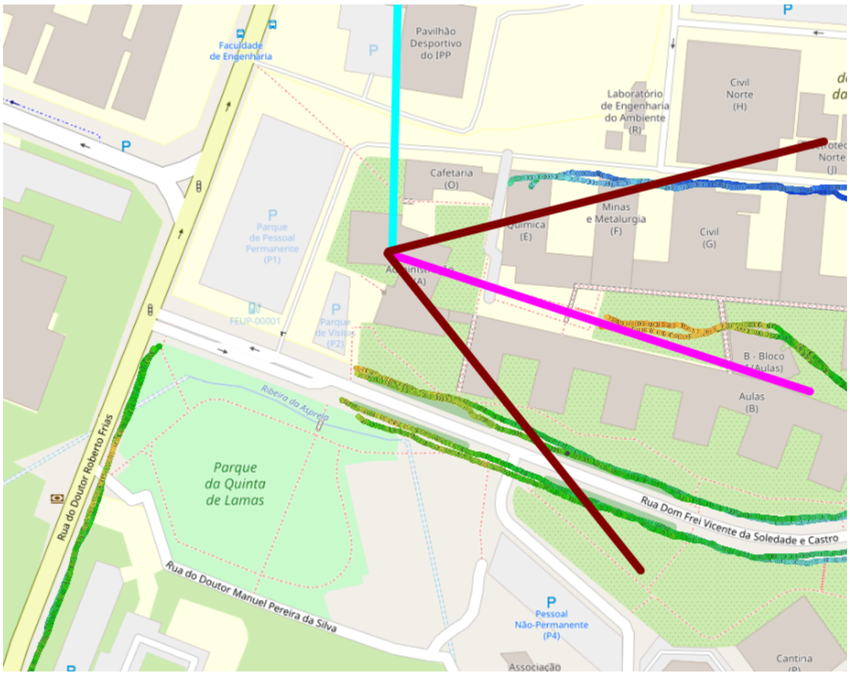

(a) 4G graph.

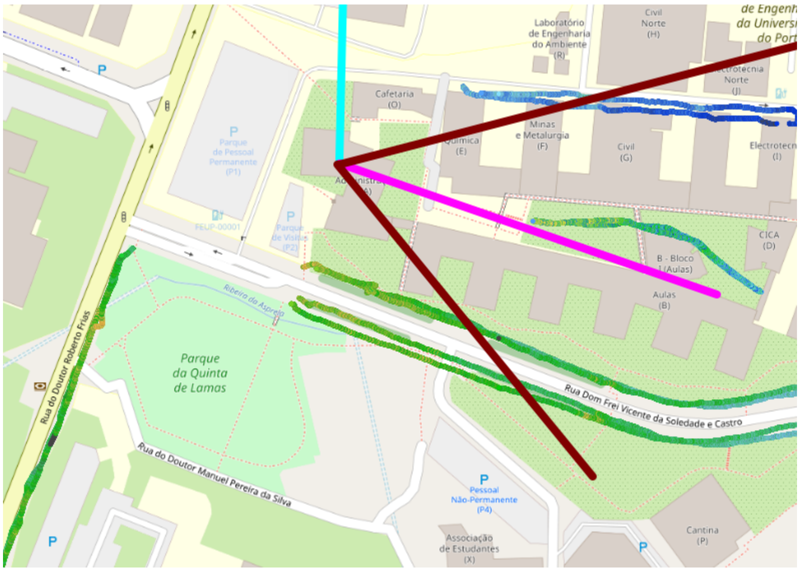

(b) 5G graph.

Figure 4.1: RSRP georeferenced plots for outdoor scenarios.

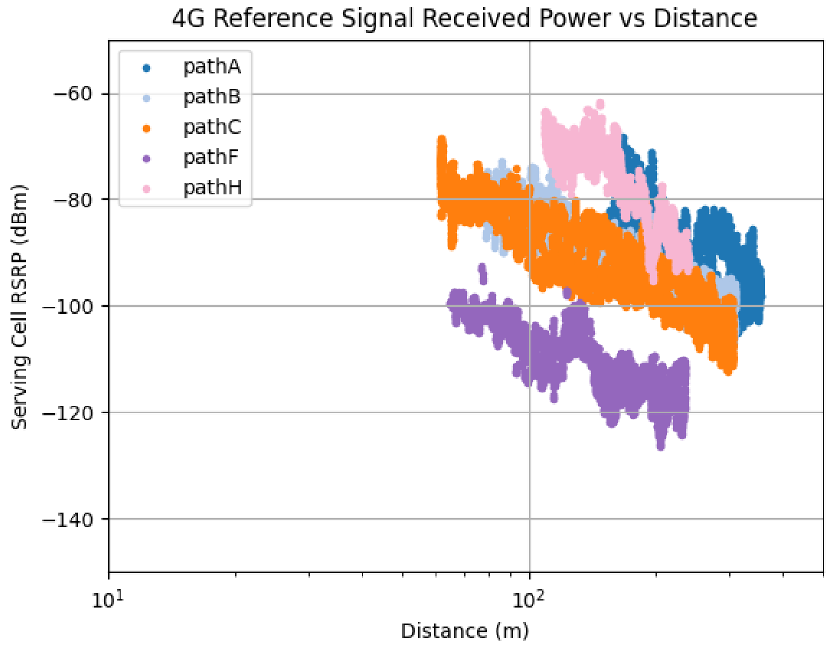

(a) 4G Plot.

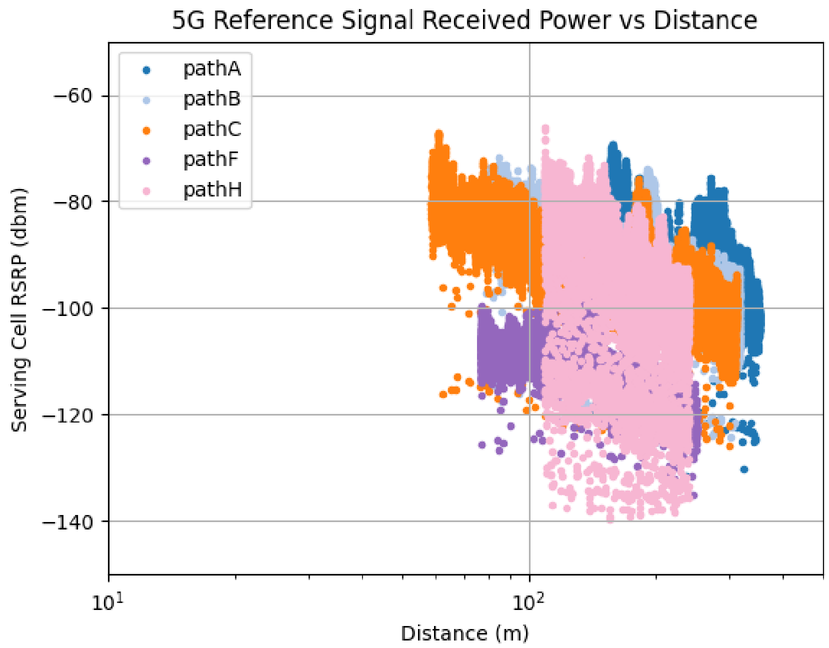

(b) 5G Plot.

Figure 4.2: RSRP versus distance for outdoor scenarios.

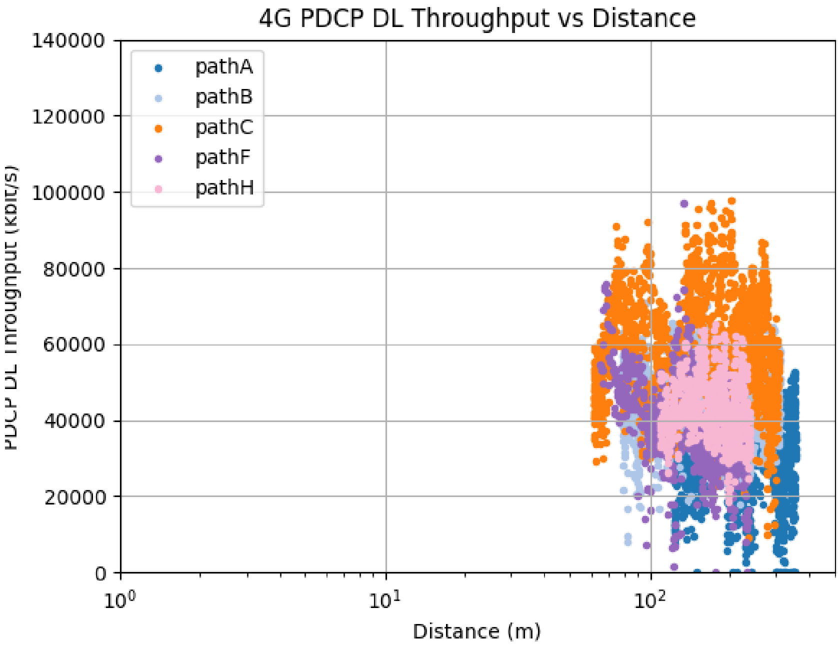

(a) 4G Plot.

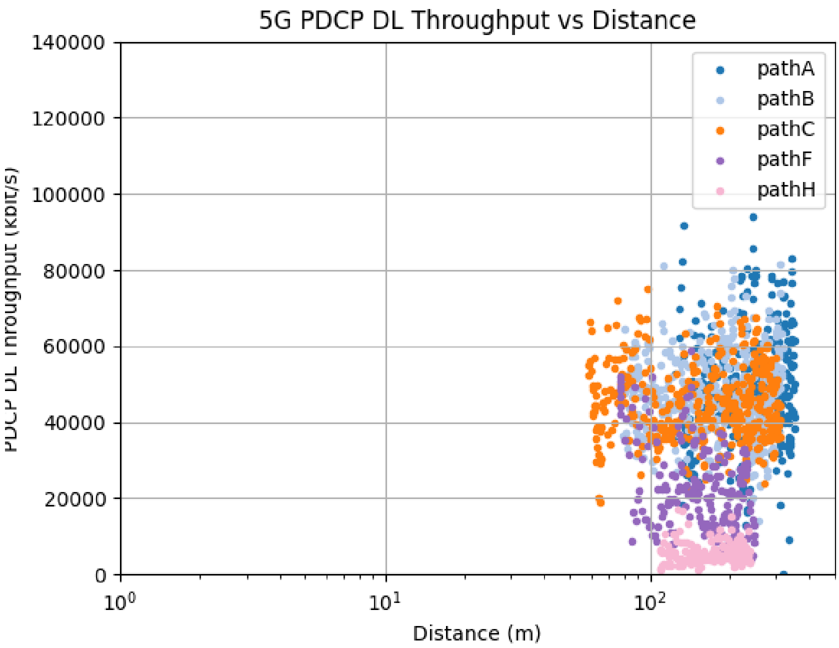

(b) 5G Plot.

Figure 4.3: Throughput versus distance for outdoor scenarios.

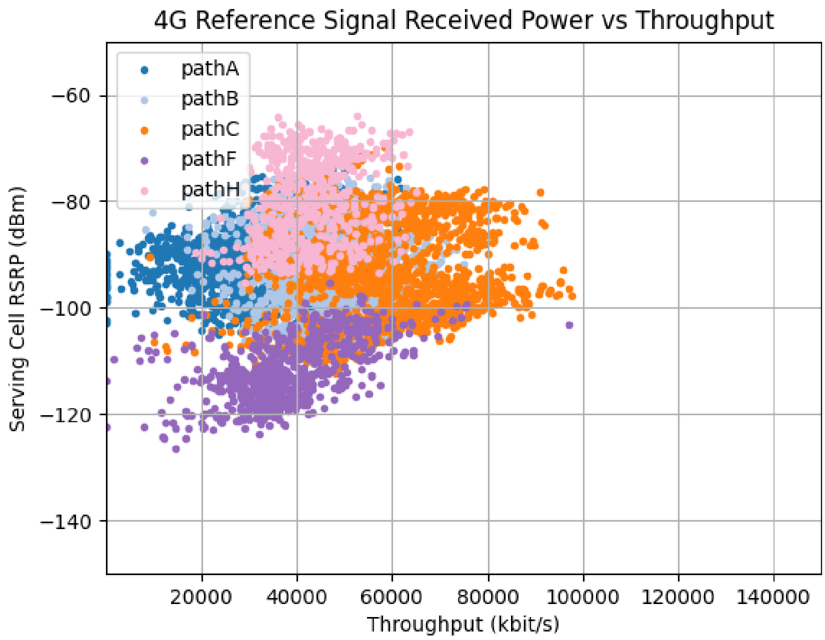

(a) 4G Plot.

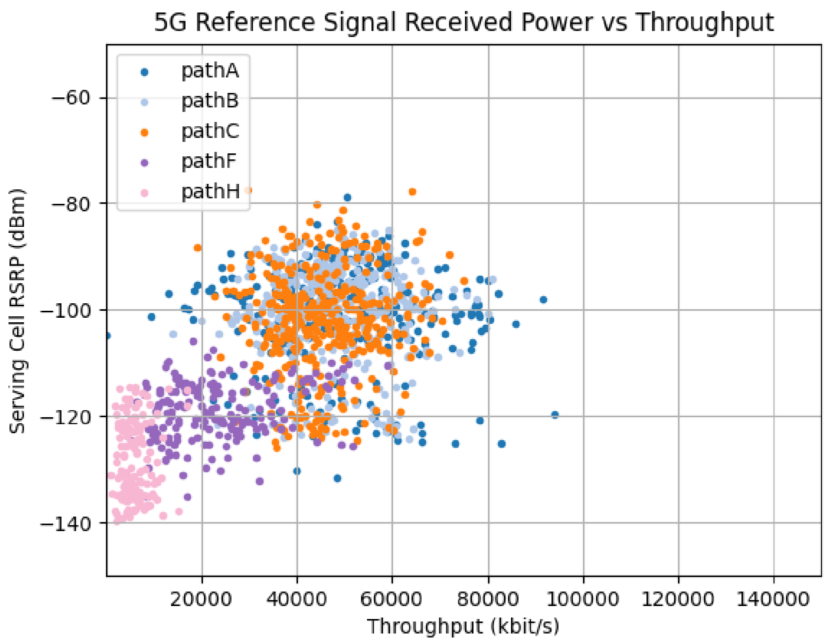

(b) 5G Plot.

Figure 4.4: RSRP versus throughput for outdoor scenarios.

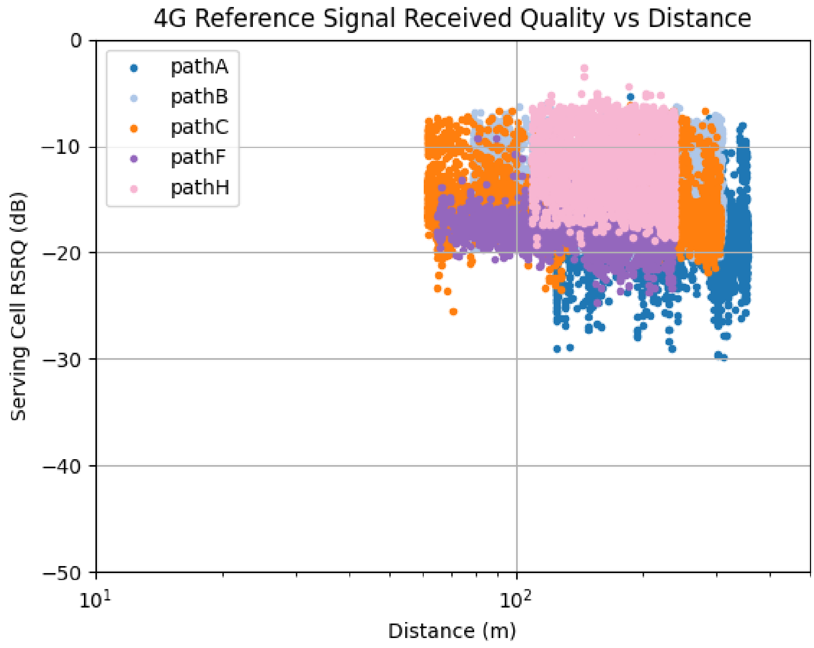

(a) 4G Plot.

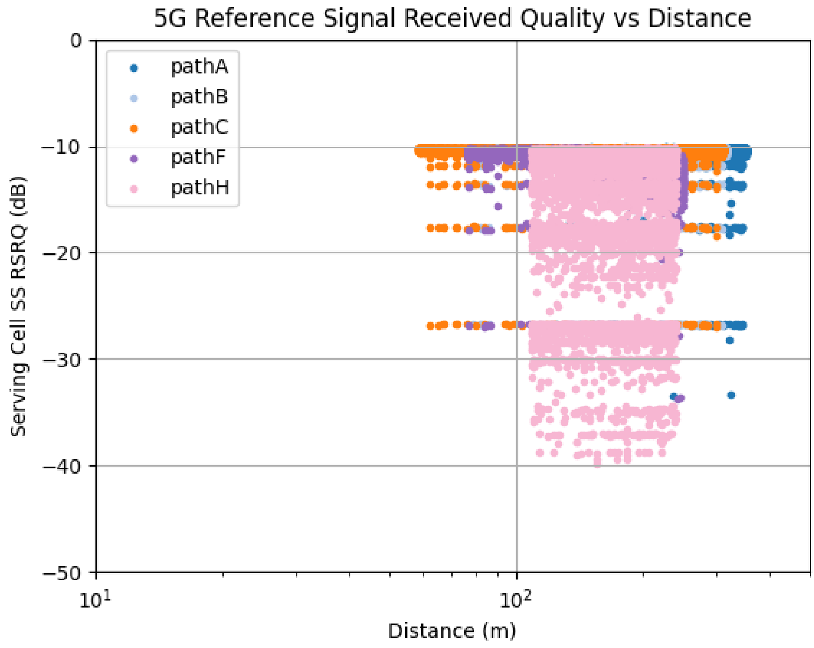

(b) 5G Plot.

Figure 4.5: RSRQ versus distance for outdoor scenarios.

4.1.2 Indoor scenarios

Paths D, E and G are located inside buildings.

Out of the blue, these results are not that straightforward to draw conclusions. As before, it was expected for the received power values to decrease as distance goes by. By looking at the graph, despite that being true, this difference is not very significant. This is even more significant in paths E and G, the first one whose data is scarce, even failing to have values for lower distances, which were expected to be the ones with the highest value, and the latter whose values oscillate following an inverted parabola function.

By observing the georeferenced plot in Figure 4.11 one can sense the fact that, albeit the measurements were made in the pre-established locations, the heatmap locates the smartphone outside, in the college garden. This can be easily interpreted due to the fact that inside buildings the GPS signal is weaker and therefore there is a higher probability of obtaining positioning errors. For this reason, we show the results plotted versus time in Fig 4.6 to make the differences between different levels perceptible.

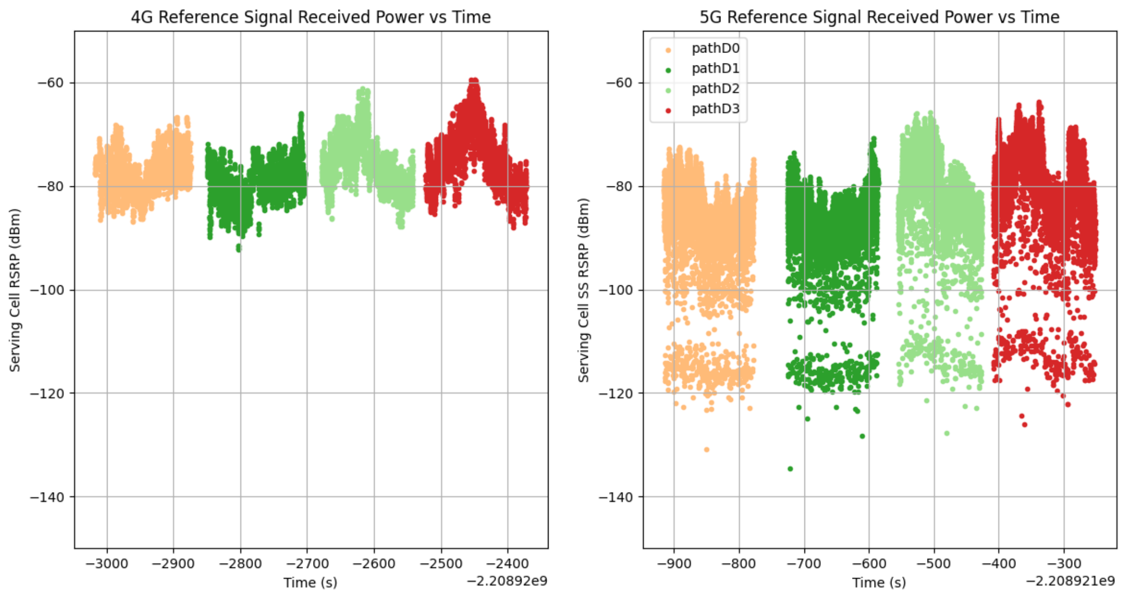

Figure 4.6: RSRP versus time for path D.

With the time plots, further conclusions can be attained. Starting with path D in Figure 4.6, as the floor level increases, it is noticeable an improvement in the values. Observing the maximum value of each path clearly shows this tendency. The parabolic evolution of the graph is justified by the fact that the path used is bidirectional so that the beginning and the end of the route coincide.

This starting and ending point is located in the farthest place in the path, for that reason the middle point for each graph corresponds to the middle point in the path. Despite the fact that it is expected for the power correspondent to shorter distances to be the biggest, for floors 0 and 1, due to concrete wall obstruction, this value is really low. For the higher floors, 2 and 3, due to the presence of a glass window by the end of the hallway, the obstruction via concrete is not observed and the interference of the glass is not as impacting on the signal as can be easily observed in Figure 4.6.

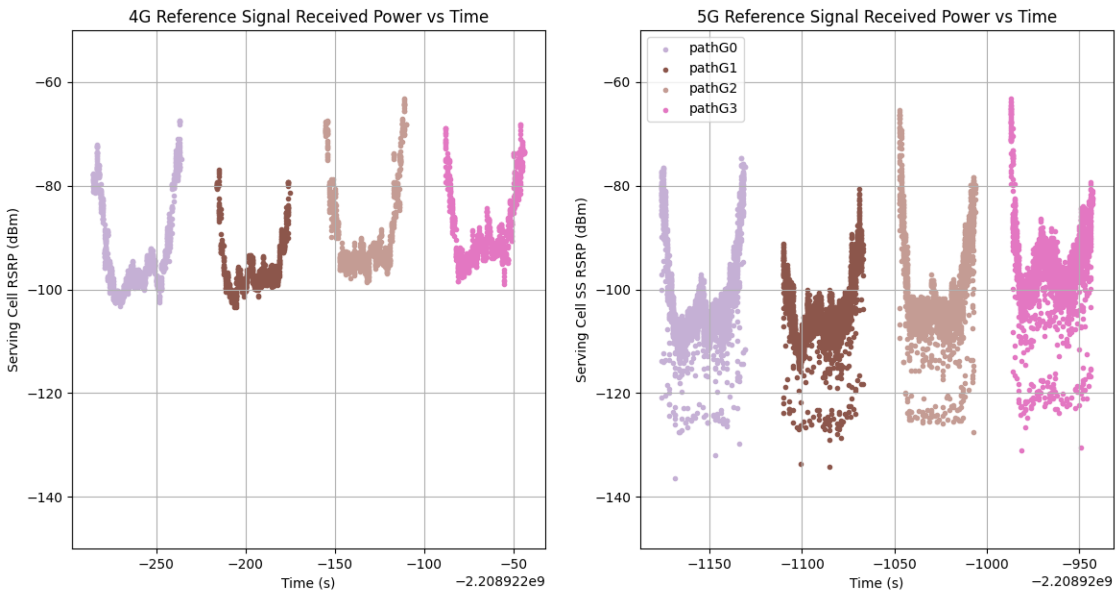

Figure 4.7: RSRP versus time for path G.

Path G is intrinsically related to path D as they are orthogonally positioned to each other. The effect of building obstruction is even more visible in this case due to the graphs (Figure 4.7) W shape in which each maximum value in each vertex correspond to a position where windows are located. In the middle point of each measurement, there is a slight increase in the power value significant to the position, yet not nearly close to the maximum values in the plot. Even though there is a window, the signal in that region suffers from shadowing due to the presence of a nearby building which helps to understand the reason behind that subtle increase.

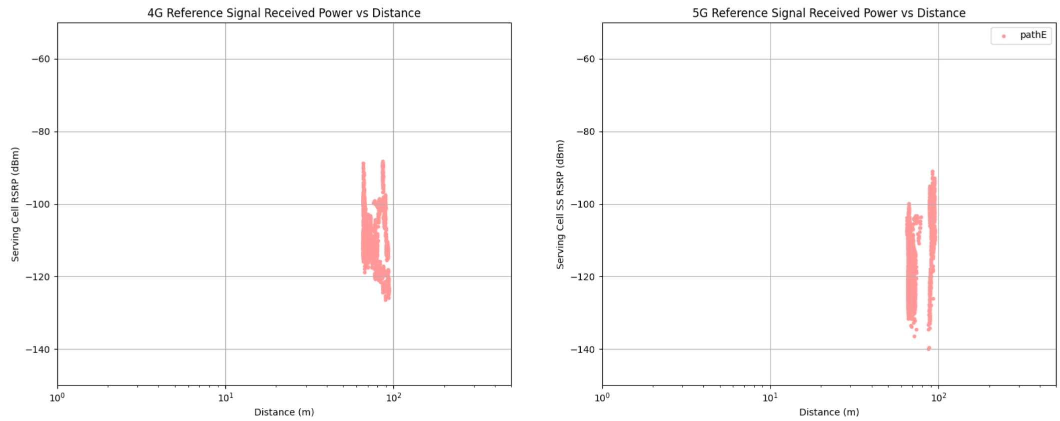

Figure 4.8: RSRP versus distance for path E.

Figure 4.9: RSRP versus time for path E.

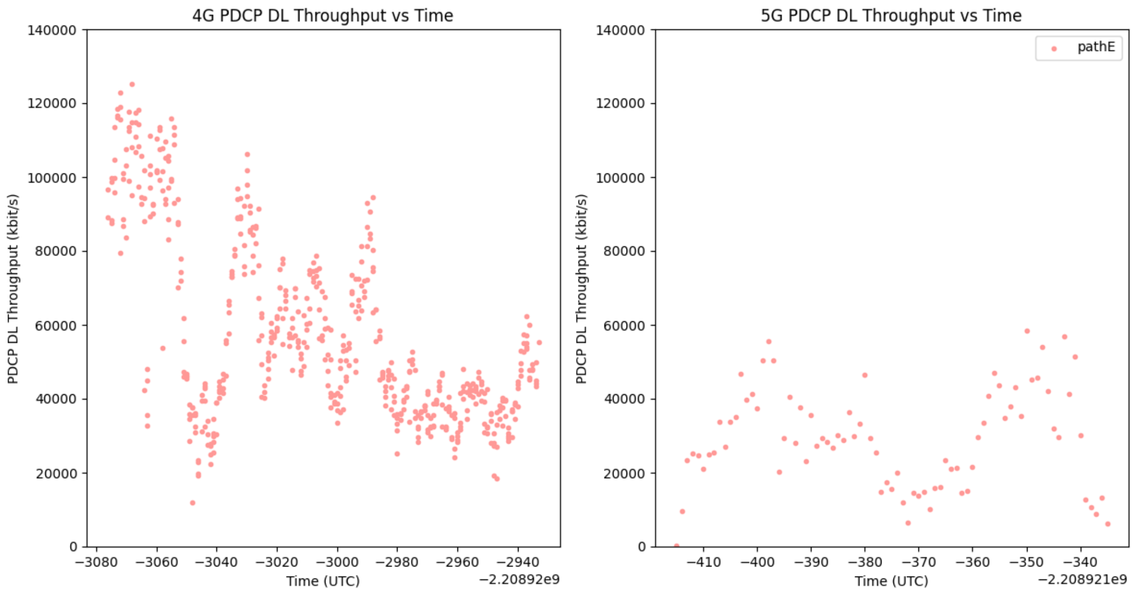

Figure 4.10: Throughput versus time for path E.

The information obtained via the measurements in path E is the one where the difference between 4G and 5G is more visible. Whereas in the previous situations the 5G plot is noticeably similar to its 4G counterpart, albeit more sparse, in this case there is a sharp difference in the observed results. For the same reasons previously mentioned, due to location errors, the RSRP versus time plot may help by providing more accurate information. In fact, the graph in Figure 4.9 helps to understand that the empty points in Figure 4.8 had information regarding RSRP which was not displayed in the graph due to the lack of georeferenced coordinates. Furthermore, observing the throughput versus time plot in Figure 4.10 this difference between 4G and 5G is even more accentuated. There are some spikes in the graph with points with considerable throughput values and others where the values are close to zero. By direct comparison of both technologies, the difference in the values is immense with the maximum throughput value measured for 5G being half of its 4G counterpart. Overall, the performance of 4G in this path is much more superior than 5G.

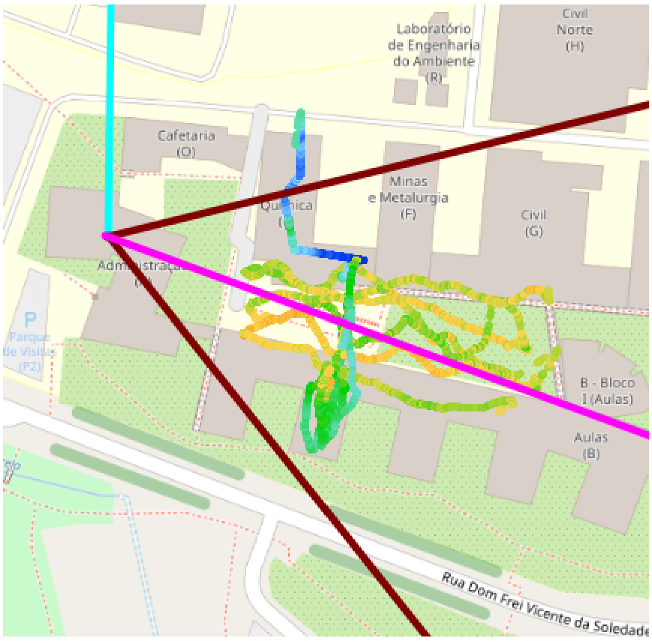

(a) 4G graph.

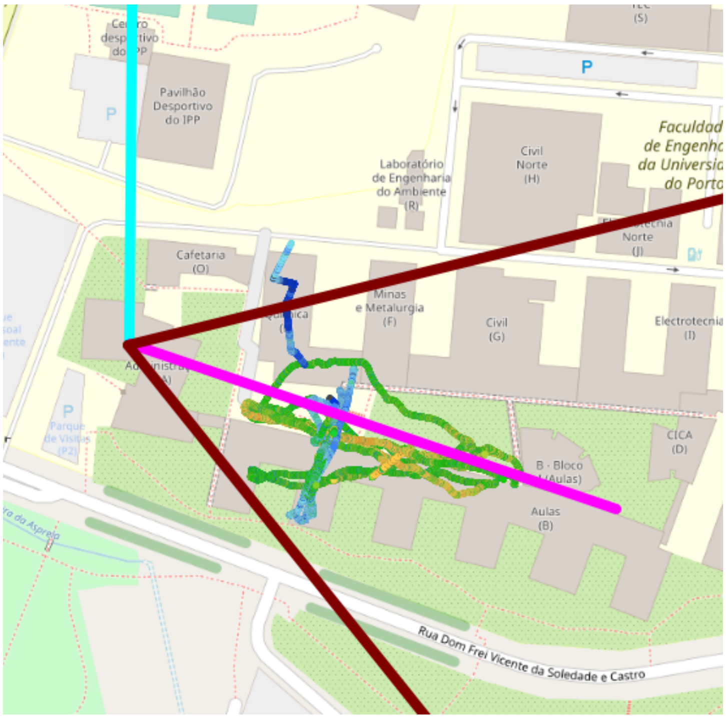

(b) 5G graph.

Figure 4.11: RSRP georeferenced plots for indoor scenarios.

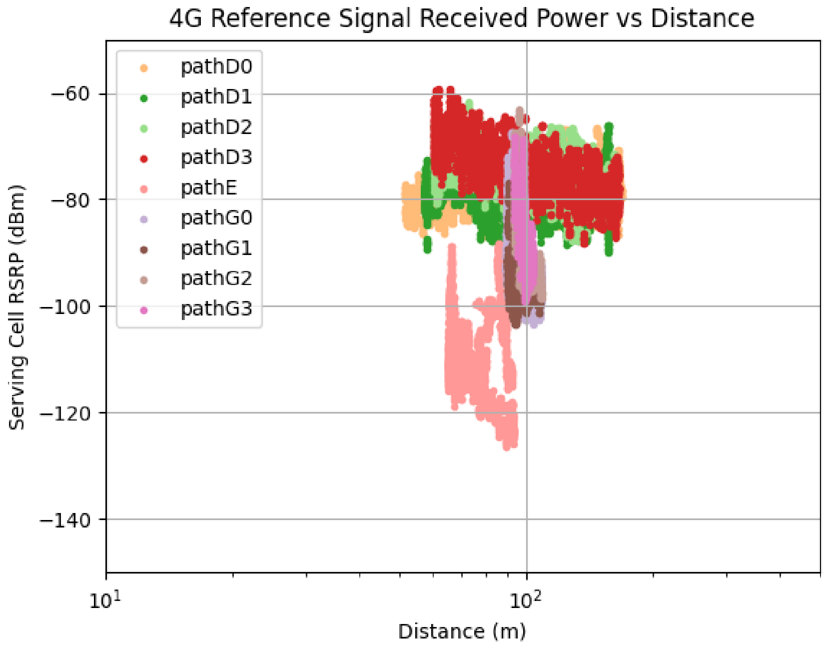

(a) 4G Plot.

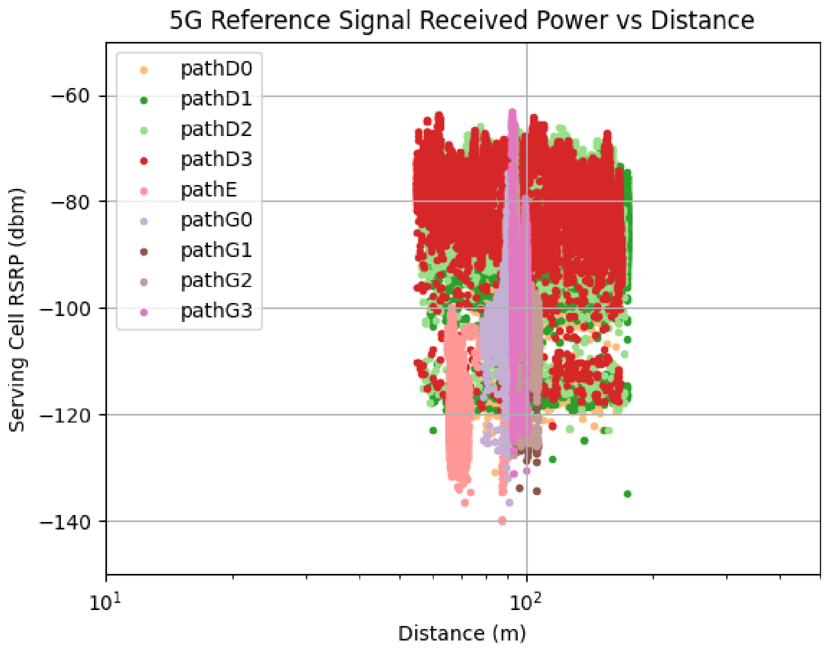

(b) 5G Plot.

Figure 4.12: RSRP versus distance for indoor scenarios.

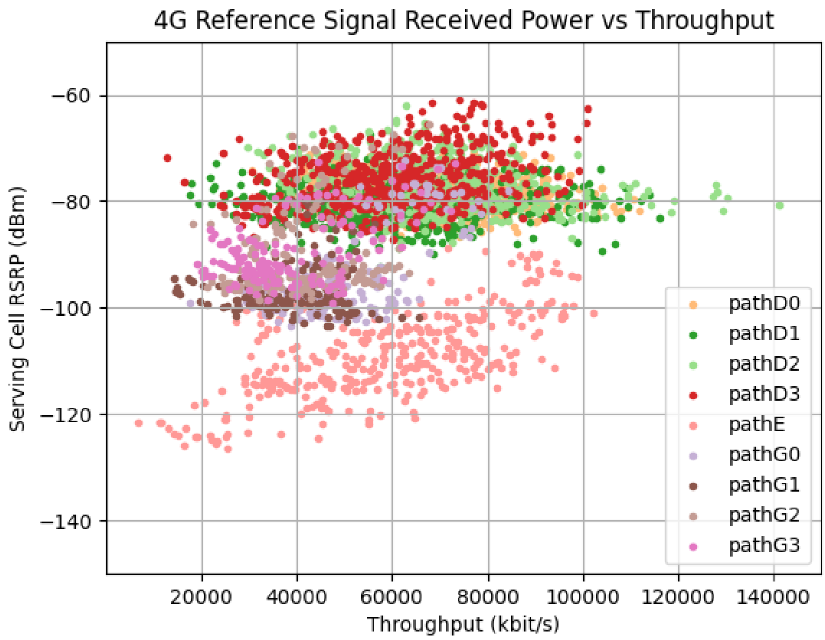

(a) 4G Plot.

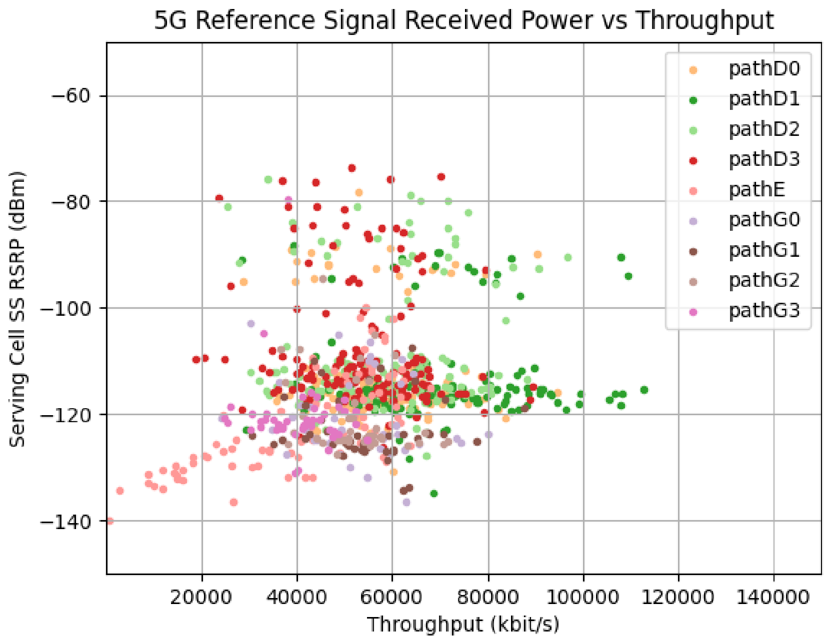

(b) 5G Plot.

Figure 4.13: RSRP versus throughput for indoor scenarios.

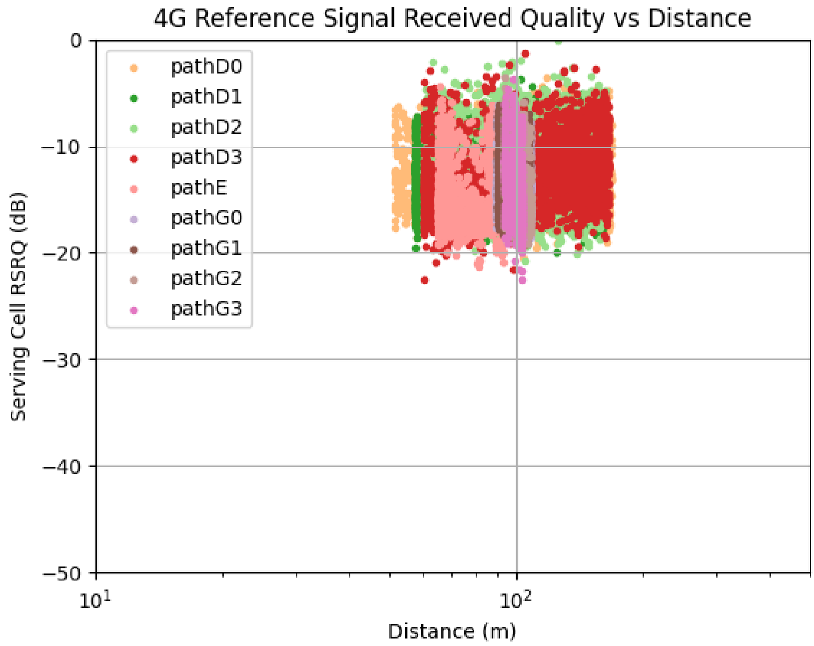

(a) 4G Plot.

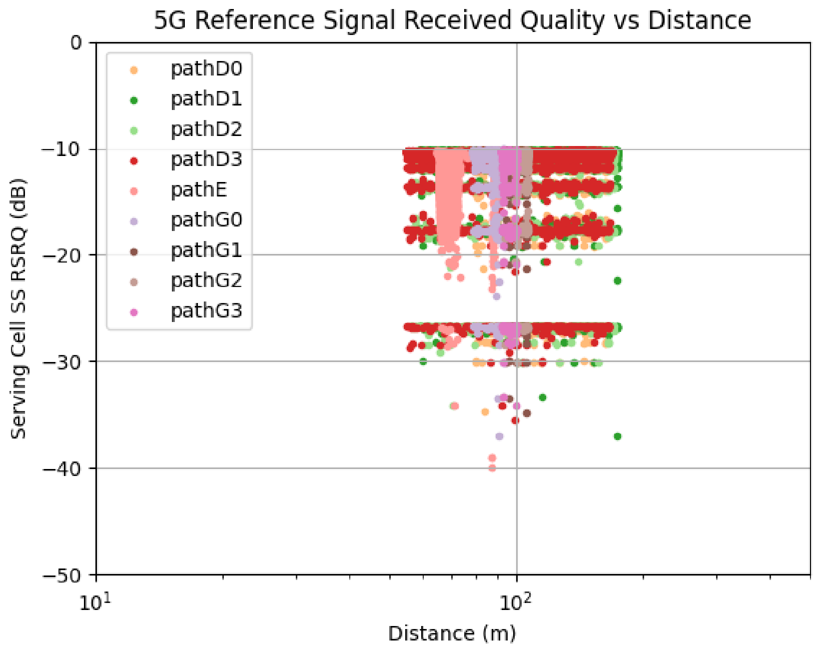

(b) 5G Plot.

Figure 4.14: RSRQ versus distance for indoor scenarios.

4.1.2.1 Indoor mapping

(a) 4G graph.

(b) 5G graph.

Figure 4.15: RSRP georeferenced plots for indoor scenarios (no geolocation errors.)

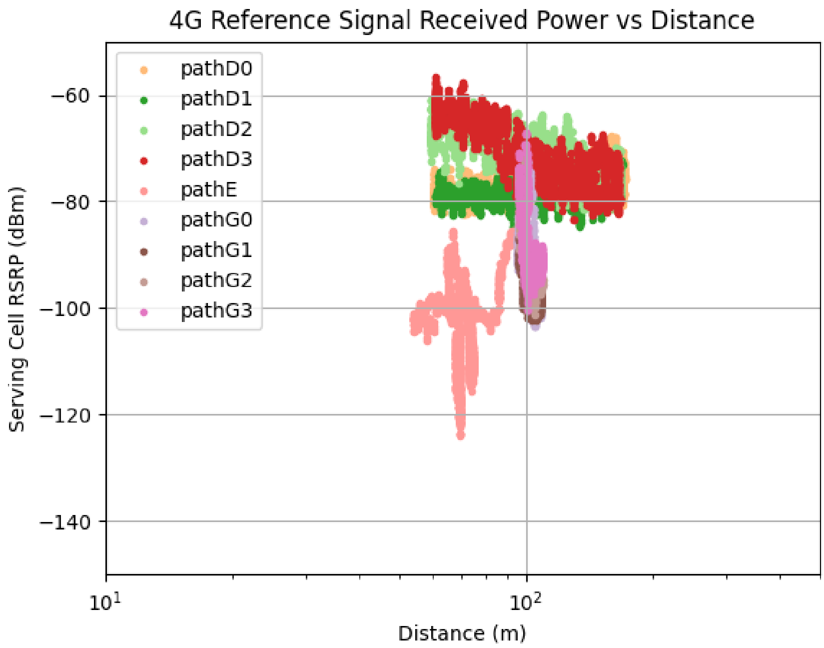

(a) 4G Plot.

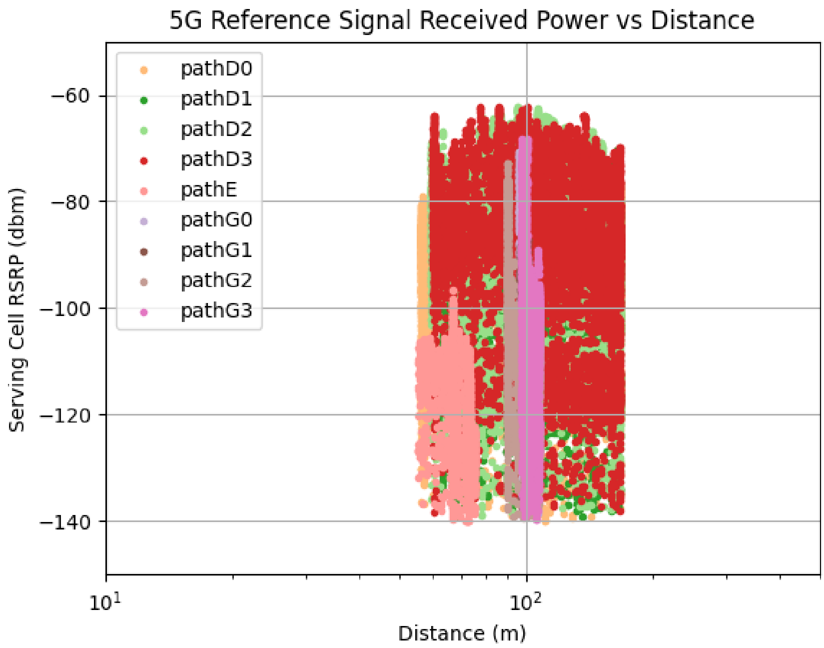

(b) 5G Plot.

Figure 4.16: RSRP versus distance for indoor scenarios (no geolocation errors).

In order to overcome the problems inherent to the GPS location errors, a new set of measurements was made, this time ignoring the GPS signal that the smartphone received. By previously drawing a map of the course, this set of measurements were made by indicating to the software the location manually by specifying, for each instant, where on the map the correspondent coordinates belong to. This way, the geolocation errors could be counterbalanced and obtain more accurate information concerning the metrics for each point. The graphical plot of RSRP versus distance for this new set of measurements is shown in Figure 4.16.

Comparing Figure 4.12 with Figure 4.16 one can assess that, despite the difference for some paths such as D2 or D3 not being very acute, for paths E and G it is more relevant in a way which grants a continuous amount of information for the measured distances. When observing Figure 4.12 and Figure 4.16 the impact of these errors is easily understood in the fact that in the latter the points correspond more accurately to those initially planned in Figure 3.1. It is when relating, separately, the throughput with both the distance and the RSRP (Figure 4.17 and Figure 4.18) that the difference between 4G and 5G is more accentuated. In Figure 4.18 the three different paths can be easily identified with path D scoring higher RSRP values for lower throughput values followed by path G and finally path E. In 5G, however, this difference is not easily perceivable with the RSRP values being 40 dB less than the 4G counterpart and the throughput values being approximately half than in 4G. In figure 4.17, this is more apparent with the 5G values falling behind the 4G ones by a large margin, despite a slight increase in the values for specific distances in both path E and G.

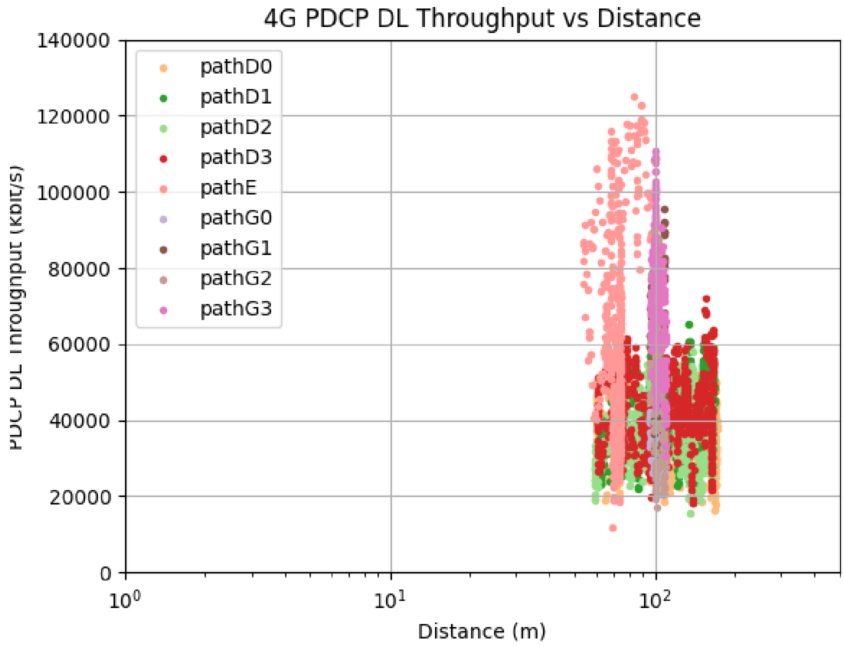

(a) 4G Plot.

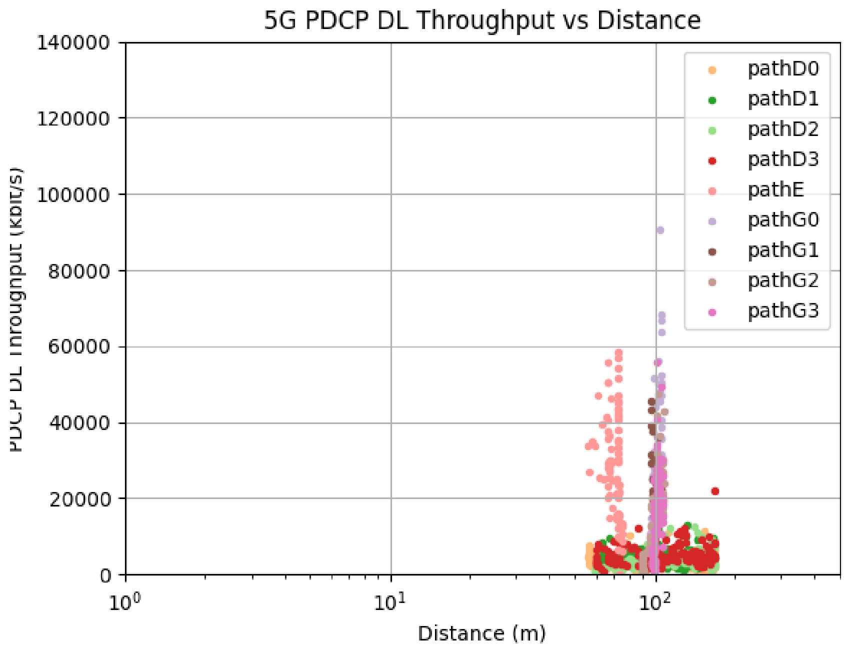

(b) 5G Plot.

Figure 4.17: Throughput versus distance for indoor scenarios (no geolocation errors).

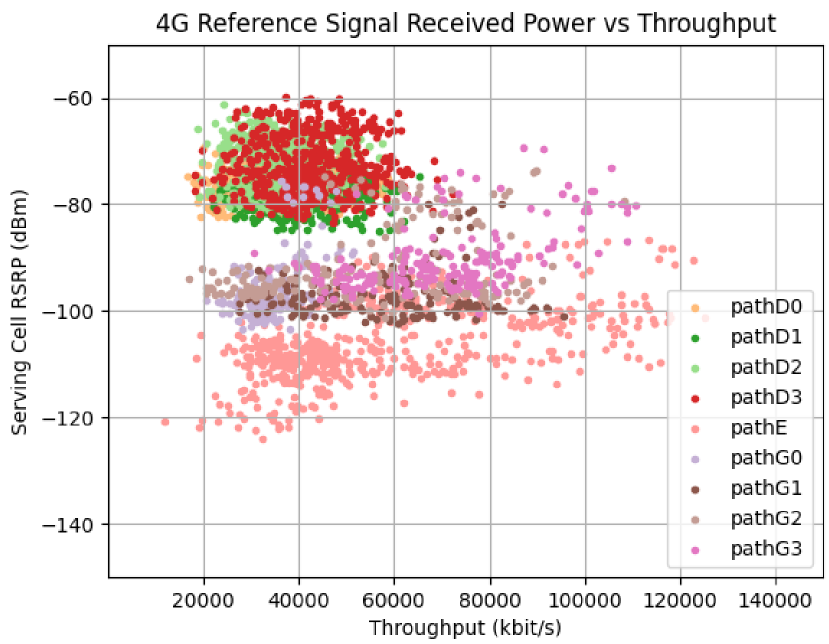

(a) 4G Plot.

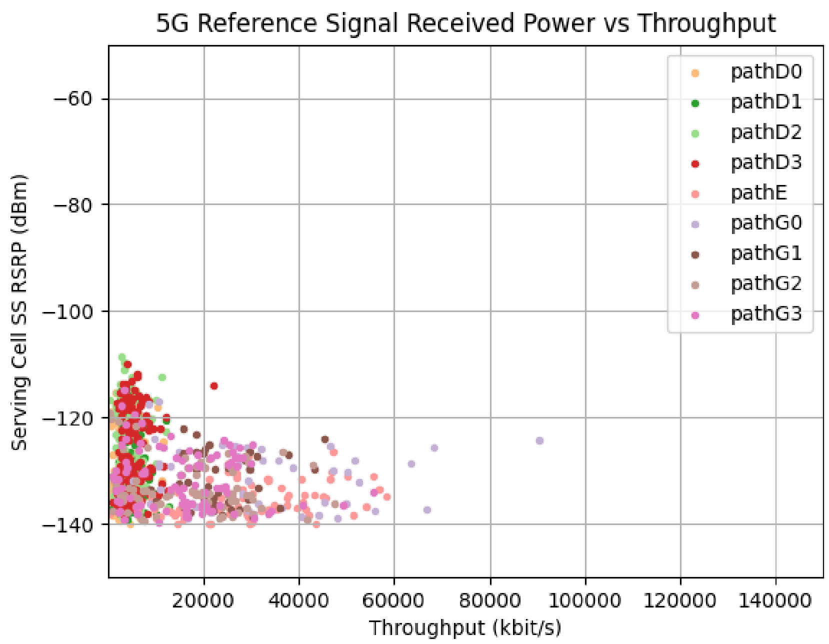

(b) 5G Plot.

Figure 4.18: RSRP versus throughput for indoor scenarios (no geolocation errors).

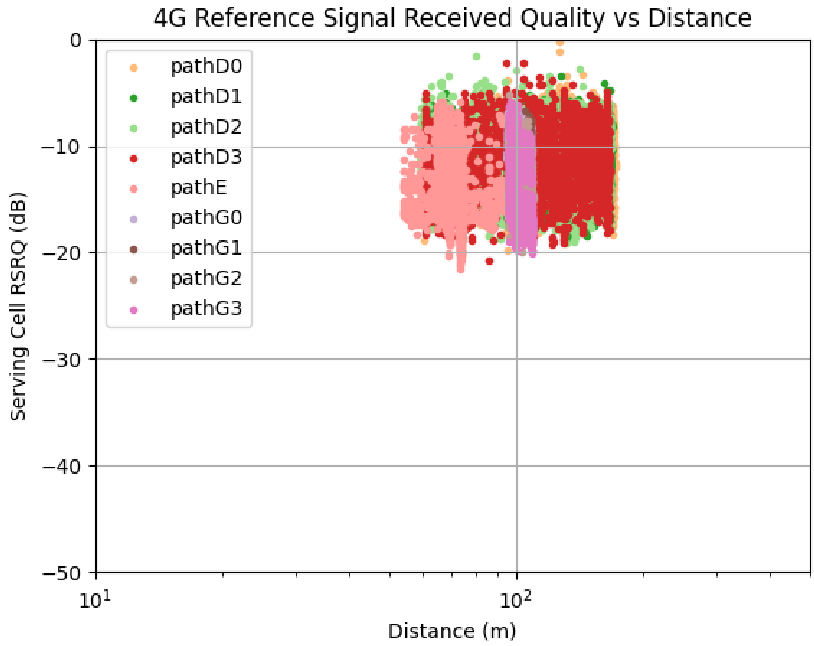

(a) 4G Plot.

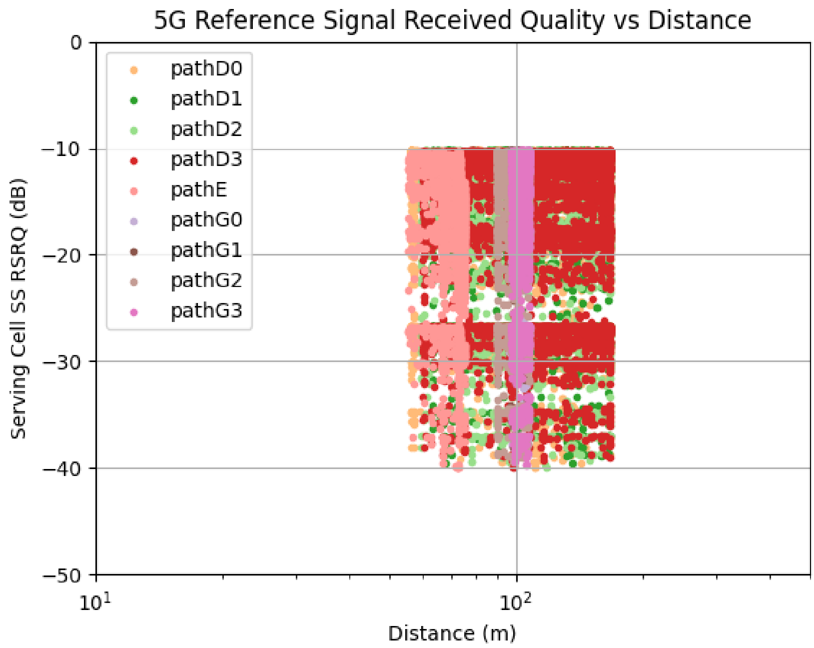

(b) 5G Plot.

Figure 4.19: RSRQ versus distance for indoor scenarios (no geolocation errors).

4.2 Modeling

On its own, the previous set of measurements, despite being a noteworthy way of reaching conclusions related to what was expected to happen in each scenario, are not alone sufficient to predict the behaviour for large distances or to establish a reference to be used in similar scenarios. Therefore, the subsequent part of this work comprises of, using the results in the previous section, employing a series of models which can quantify those results.

4.2.1 Linear regression analysis

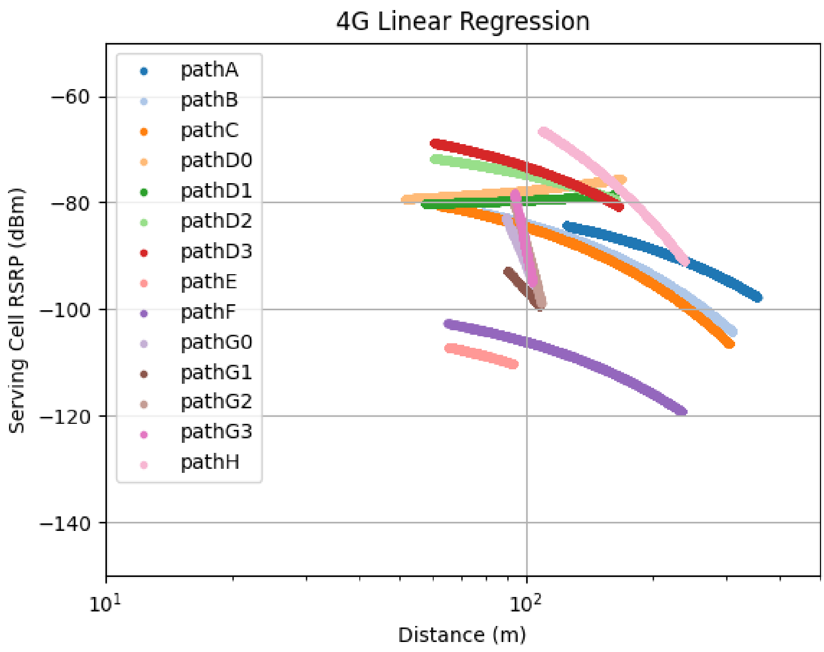

(a) 4G Plot.

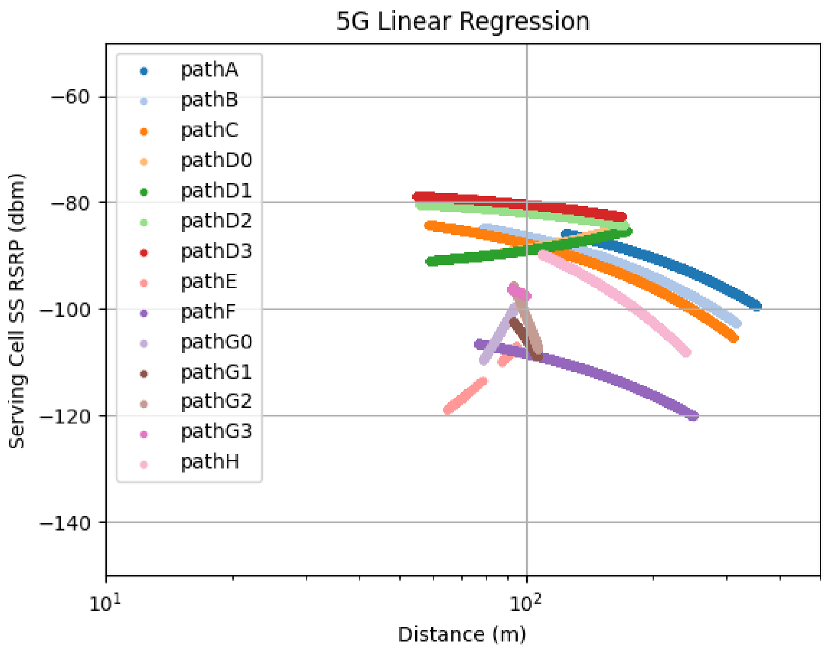

(b) 5G Plot.

Figure 4.20: Linear functions of RSRP versus distance.

Paths	Coefficient of determination (R^2)	Intercept (b0 coefficient)	Slope (b1)
A	0.332	-22.912	-28.852
B	0.813	-6.758	-38.269
C	0.822	-9.227	-37.984
F	0.665	-41.900	-32.089
H	0.814	-45.681	-0.190

Table 4.1: Linear regression parameters for outdoor 4G scenarios

Paths	Coefficient of determination (R^2)	Intercept (b0 coefficient)	Slope (b1)
A	0.298	-25.753	-28.345
B	0.620	-25.769	-30.034
C	0.662	-27.426	-30.335
F	0.461	-57.077	-25.620
H	0.144	-74.399	-0.140

Table 4.2: Linear regression parameters for outdoor 5G scenarios

The equations in the models mentioned in chapter 2 can be solved in a way that can be traced to a linear regression. For that reason, it is extremely relevant for this process to be made. The linear regression parameters can be found in Table 4.1, and Table 4.2. The explanatory variable is the distance in logarithmic scale and the dependent variable is the RSRP.

4.2.1.1 Outdoor scenarios

The slope variation for paths B, C and F is unmistakably small between them. This is interesting as a way of modelling the interference of buildings for similar conditions. Contrasting with the other outdoor paths, the 4G and 5G regressions for path H are not proportional with the other four. The signal power in 5G is significantly worse.

4.2.2 Propagation models

Using the free space path loss formula, one gets the following:

$$P_R[dB] = P_T[dB] + G_T(\theta,\phi)[dB] + G_R[dB] - PL[dB] \tag{4.1}$$

where P_R and P_R are the received and transmitted power, respectively, G_R and G_T are the received and transmitted gain, respectively, and *PL* is the path loss. Considering that the values of P_T and G_R are constant for each measured point and that the value of G_T varies for each measured location, specially those located outside the antenna's main lobe, this value needs to be taken into account when performing calculations. Therefore, one can assume for a new variable which we call Pr^c to be the difference between the received power and the transmitted gain. Assuming the values of P_t and G_r in this equation to be K_1 and K_2, and subsequently subtracting the transmission antenna gain to the received power, the prior formulas can be rewritten as:

$$PL[dB] = K_1 + K_2 - Pr^c[dB] \tag{4.2}$$

As mentioned previously, the value of G_T is dependent on the location around the base station. As such, this compensation needs to be considered differently for each technology and each location. This was achieved using the propagation diagram of each antenna which supplies the value for the horizontal and vertical gain for each spot. For this reason, it is important for the distance measurement between two points to consider the altitude of the base station. Due to the fact that the measurements distance to the base station are relatively small, ranging from 50 to 500 meters, we can pretend that, for this scenario, the Earth is flat as the surface curvature value is so insignificant that it does not constitute a noticeable precision loss. So, the calculation of the distance, in meters, between the base station and the smartphone was made using the formula in equation 4.3.

$$d[m] = \sqrt{h^2 + x^2} \tag{4.3}$$

where h consists of the height of the antenna in meters and x consists of the distance between the coordinates of the smartphone and the base station. For the horizontal and vertical gains, the correspondent azimuth for each point was calculated with the previous information in mind. Considering the location and the height for horizontal and vertical gains respectively, the information for each point was compensated using the values of the propagation diagram for each technology used by the base station.

4.2.2.1 Alpha-Beta-Gamma (ABG)

The first model used was the Alpha Beta Gamma model due to its practicability. Considering the fact that in our case there is only a single frequency used for each technology (being in 4G of 1.8 GHz and on 5G of 3.5 GHz), the γ coefficient which corresponds to the dependence of path loss on frequency doesn't change for each point and its value equal to 2 correspondent to a free space scenario. Using equation 2.8 and 4.2 we obtain:

$$K_1 + K_2 - Pr^c[dB] = 10\alpha \log_{10}\left(\frac{d}{1m}\right) + \beta + 10\gamma \log_{10}\left(\frac{f}{1GHz}\right) + \chi_\sigma^{ABG} \tag{4.4}$$

Developing this equation as function of χ^{ABG} we obtain:

$$\chi_\sigma^{ABG} = -Pr^c[dB] - 10\alpha \log_{10}\left(\frac{d}{1m}\right) - \beta + K_1 + K_2 - 10\gamma \log_{10}\left(\frac{f}{1GHz}\right) \tag{4.5}$$

which can be further reduced by grouping all the constants:

$$\chi_{\sigma}^{ABG} = -Pr^{c}[dB] - 10\alpha\log_{10}\left(\frac{d}{1m}\right) - \beta'' \tag{4.6}$$

Assuming $B = PL^{ABG}(f,d)[dB]$, $D = 10log_{10}(d)$ [28], the equation of shadow fading is:

$$\chi^{ABG} = B - \alpha D - \beta'' \tag{4.7}$$

and its standard deviation is:

$$\sigma^{AB} = \sqrt{\sum(B - \alpha D - \beta'')}[28] \tag{4.8}$$

In order to calculate the values of α and β'', the following system of equations can be used:

$$\begin{cases} \alpha\sum D^2 + \beta\sum D - \sum DB = 0 \\ \alpha\sum D + N\beta - \sum B = 0 \end{cases}$$

4.2.2.2 Close-In

This model is similar to Alpha-Beta-Gamma in its implementation except it only has one parameter to be optimised. Using the equation 4.9, we can get:

$$K_1 + K_2 - Pr^{c}[dB] = FSPL(f, 1m)[dB] + 10n\log_{10}(d) + \chi_{\sigma}^{ABG} \tag{4.9}$$

Developing this equation as function of χ_{σ}^{CI} we obtain:

$$\chi_{\sigma}^{CI} = K_1 + K_2 - Pr^{c}[dB] - FSPL(f, 1m)[dB] - 10n\log_{10}(d) \tag{4.10}$$

Being $K_1 + K_2 - Pr^{c}[dB] - FSPL(f, 1m)[dB]$ represented by A and $10n\log_{10}(d)$ as D, then the shadow fading standard deviation can be rewritten as [28]:

$$\sigma^{CI} = \sqrt{\sum(a - nD)^2/N} \tag{4.11}$$

Using the formulas mentioned above, the values in the equations were calculated using the measured data and grouped in Table 4.2.2.2

		f (GHz)	d (m)	Model	α (n)	β"	σ
4G	**LOS**	1.8	110 - 355	**AB**	-7.43	73.03	196.50
				CI	3.14	—	4.31
	NLOS	1.8	55 - 309	**AB**	-2.49	-45.92	195.15
				CI	2.24	—	3.67
5G	**LOS**	3.5	109 - 353	**AB**	-3.46	-26.44	212.32
				CI	10.54	—	14.08
	NLOS	3.5	56 - 317	**AB**	0.18	-115.25	223.54
				CI	11.99	—	23.46

By observing Table 4.2.2.2 for 4G in both LOS and NLOS scenarios, the value of α in the CI model is close to the value 2 which is coherent to the path loss estimation for free space which is 2.

Chapter 5

Conclusion

5.1 Summary

In this work, a performance comparison of two broadband cellular networks technologies in different propagation scenarios has been made. The measurements collected took almost a week to be made along with several months prior where the equipment and the tools used were honed. With this data, a series of conclusions regarding each technology could be reached which served as a harbinger to what to expect with the results of the ensuing step of this work, the modelling. With that information, we could clearly see the difference in performance between indoor and outdoor scenarios, with the latter providing more clear information which was used for the modelling. Furthermore, for the same scenarios specified in this work, 4G outperforms 5G with this comparison being more evident in indoor scenarios where the performance of 5G is worse.

5.2 Future Work

The empirical and experimental characteristic of this work allows for a plethora of different ways to continue this study. There is the opportunity of developing new measurements with different atmospheric conditions in order to study its influence in the values. Regarding the modelling component of this work, only two models were used, so, a different number of other models can be used in furtherance of getting a way to predict the signal path loss and other information.

Appendix A

Appendix

A.1 Single plots for RSRP versus distance

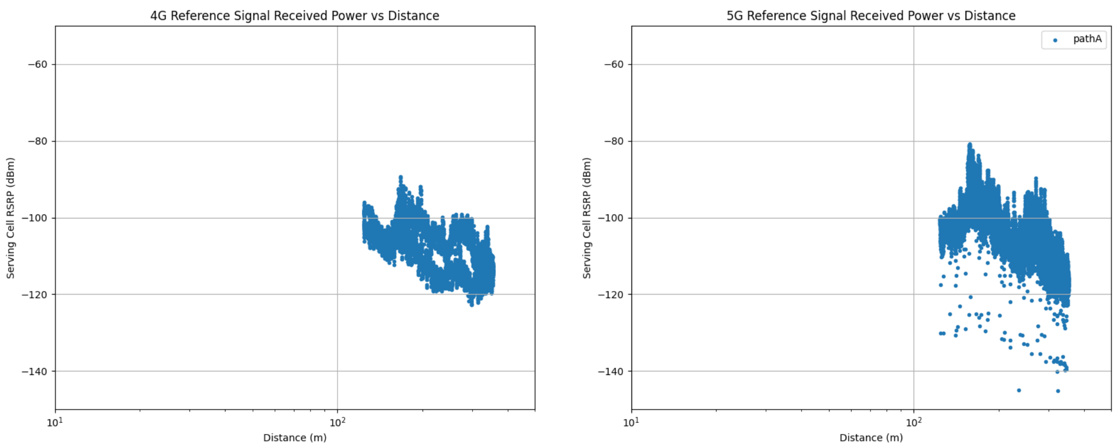

Figure A.1: RSRP versus distance for path A

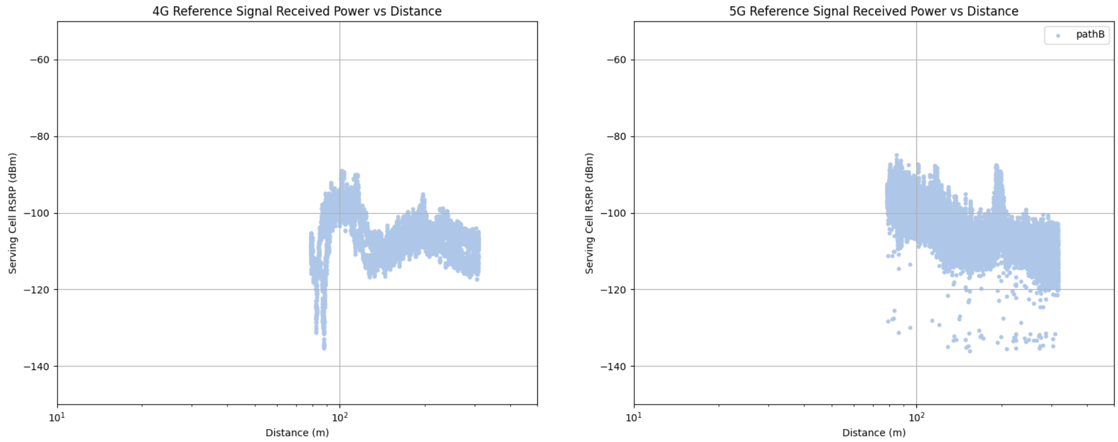

Figure A.2: RSRP versus distance for path B

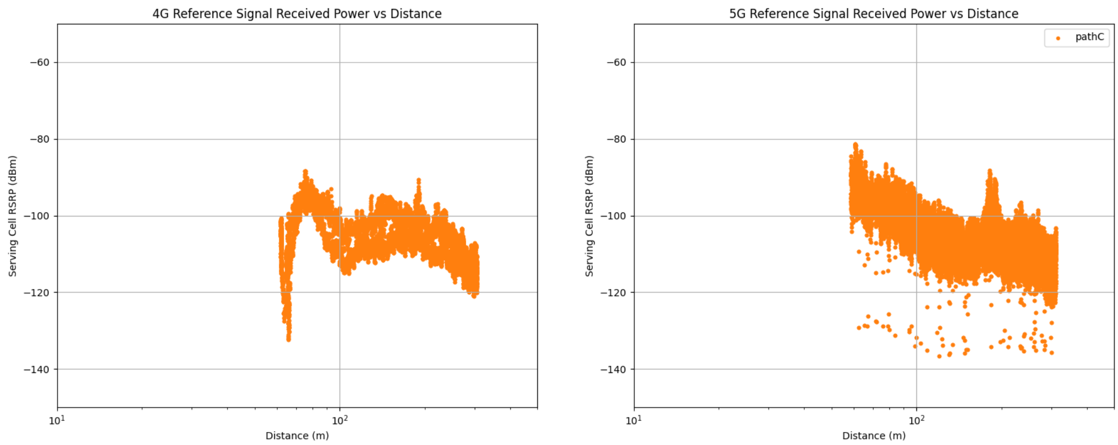

Figure A.3: RSRP versus distance for path C

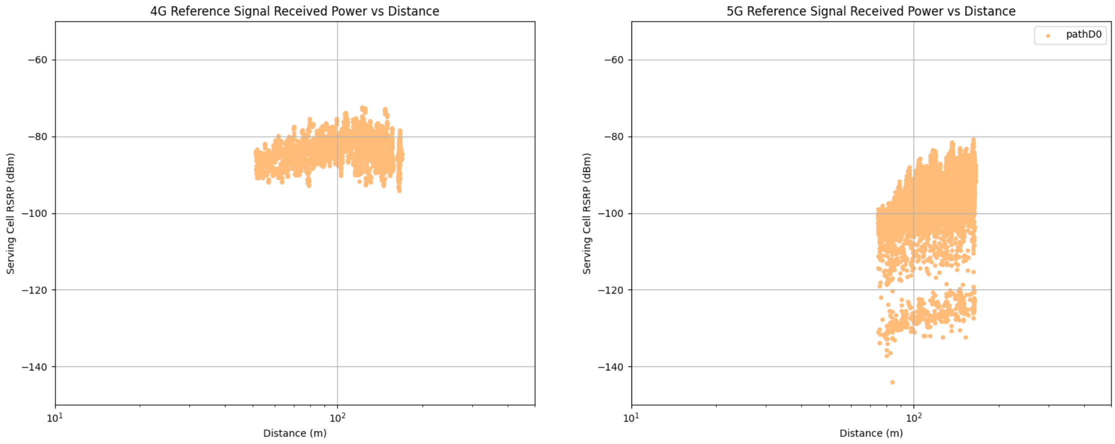

Figure A.4: RSRP versus distance for path D0

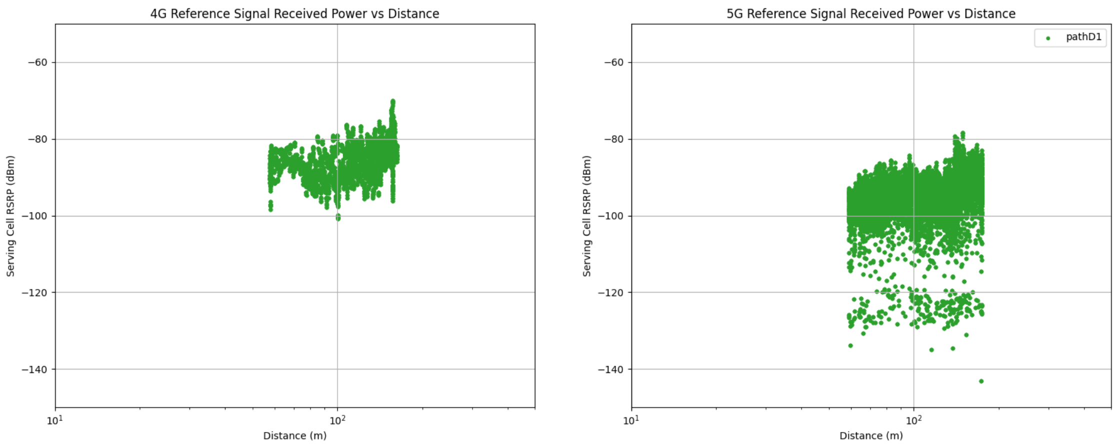

Figure A.5: RSRP versus distance for path D1

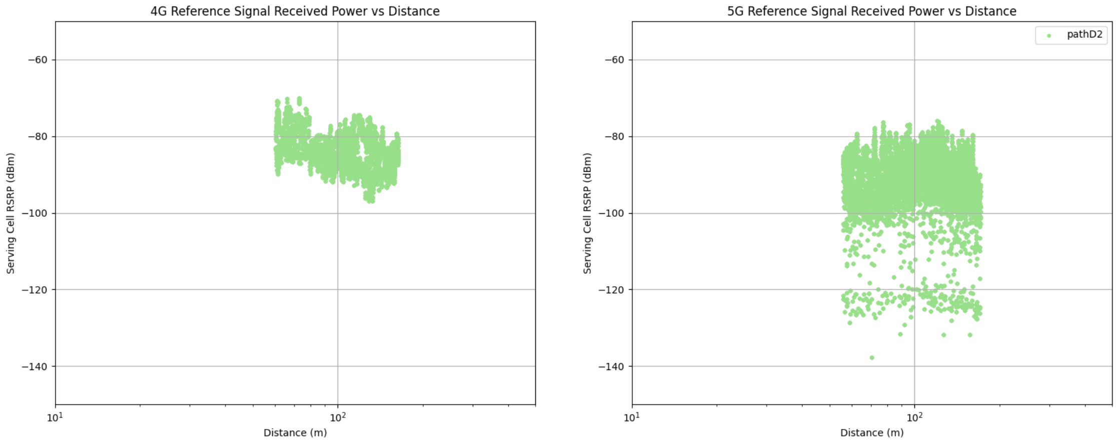

Figure A.6: RSRP versus distance for path D2

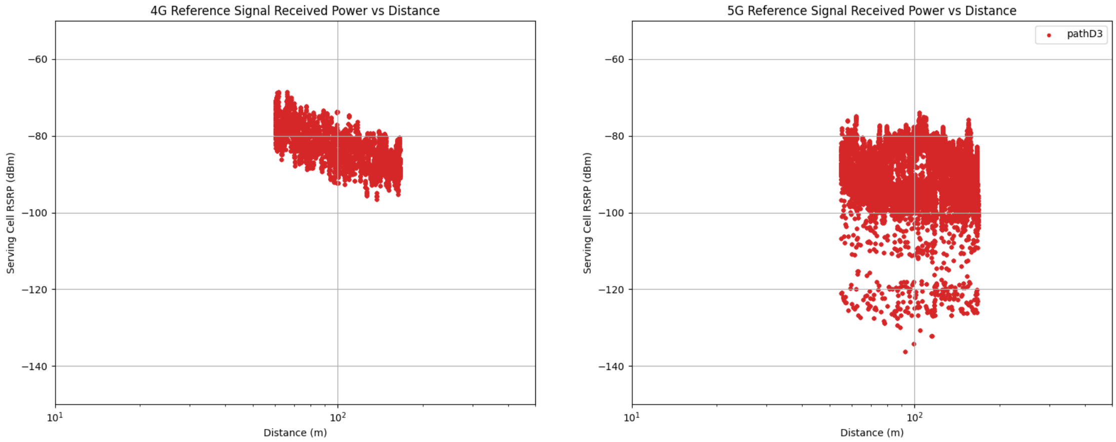

Figure A.7: RSRP versus distance for path D3

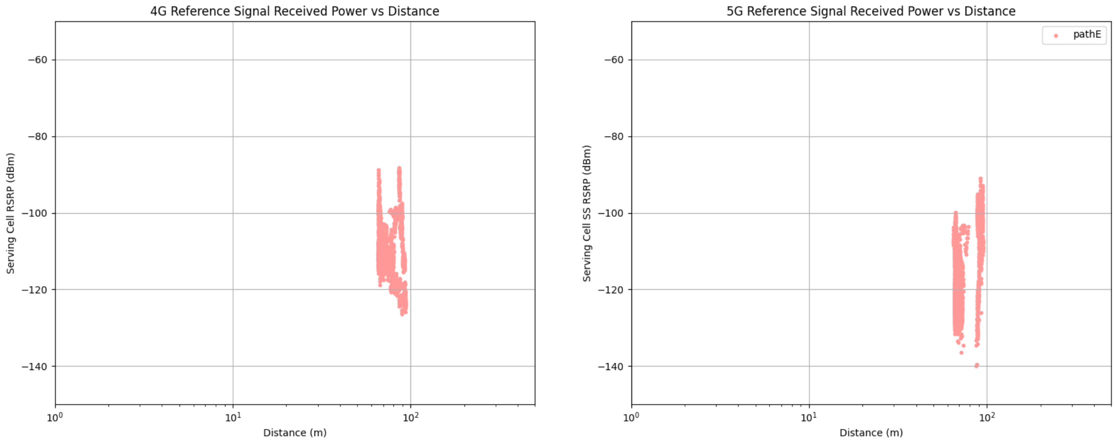

Figure A.8: RSRP versus distance for path E

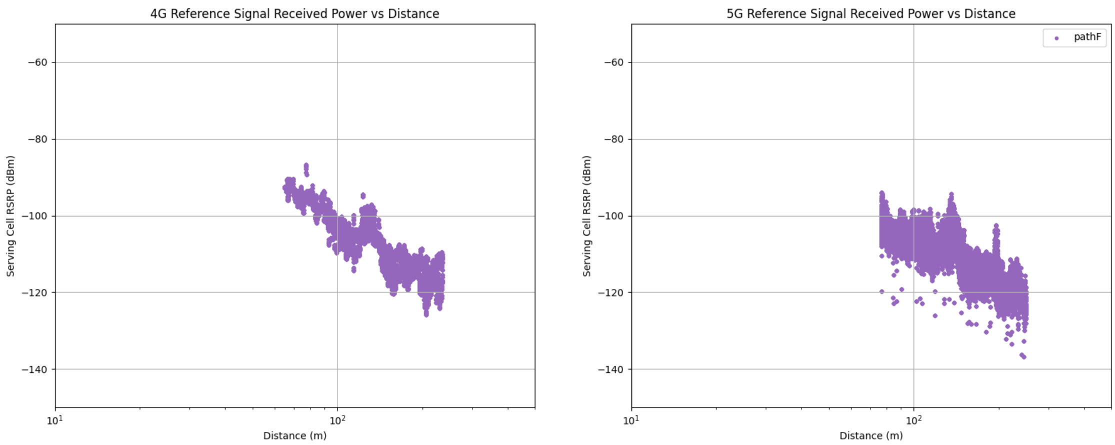

Figure A.9: RSRP versus distance for path F

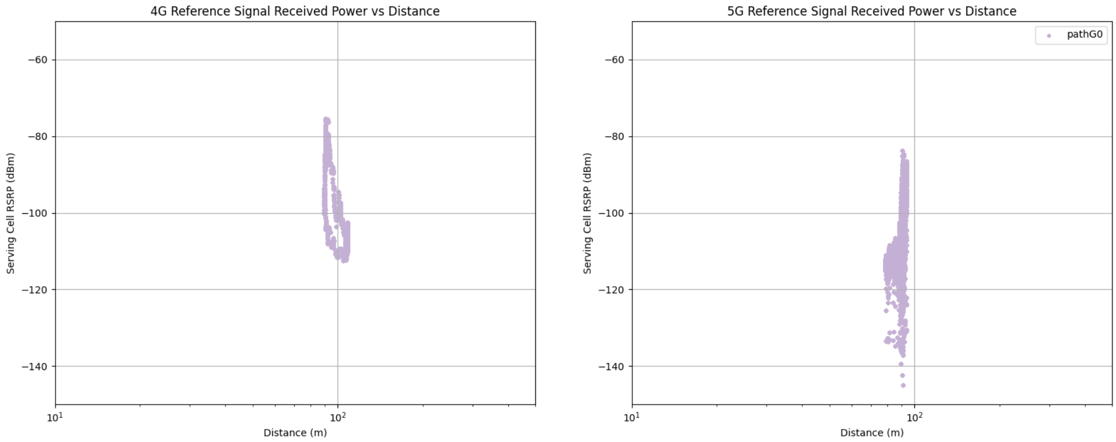

Figure A.10: RSRP versus distance for path G0

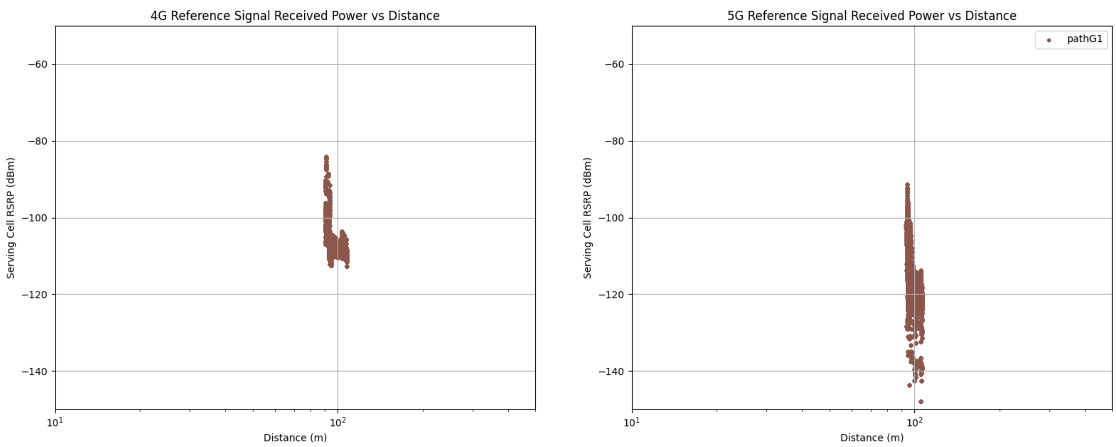

Figure A.11: RSRP versus distance for path G1

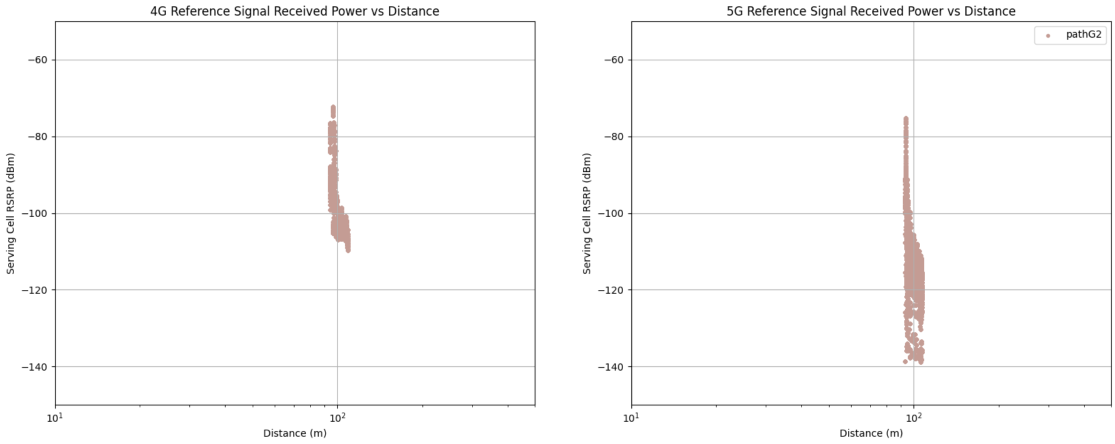

Figure A.12: RSRP versus distance for path G2

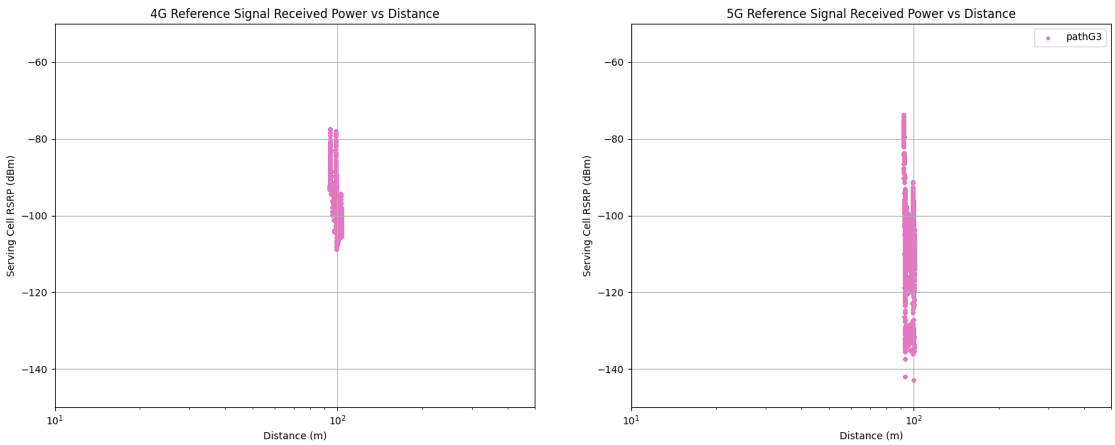

Figure A.13: RSRP versus distance for path G3

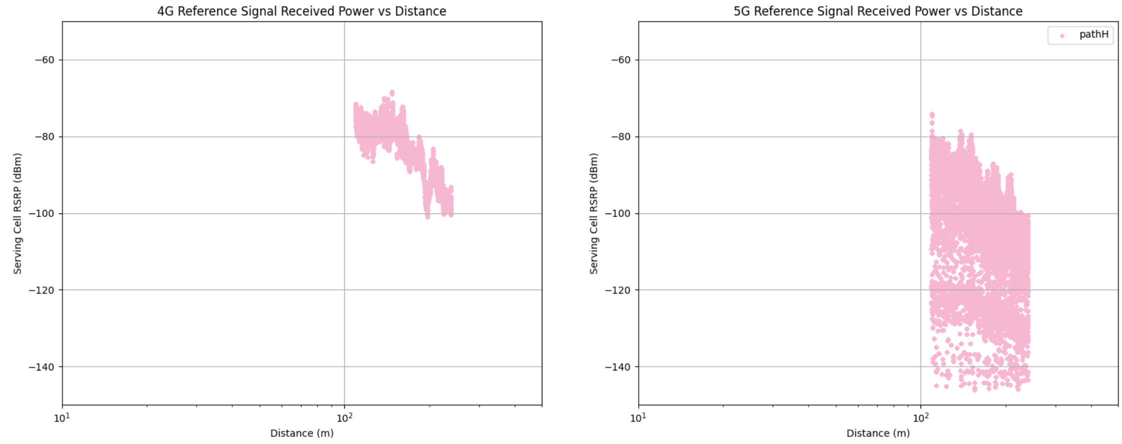

Figure A.14: RSRP versus distance for path H

A.2 Single plots for Throughput versus distance

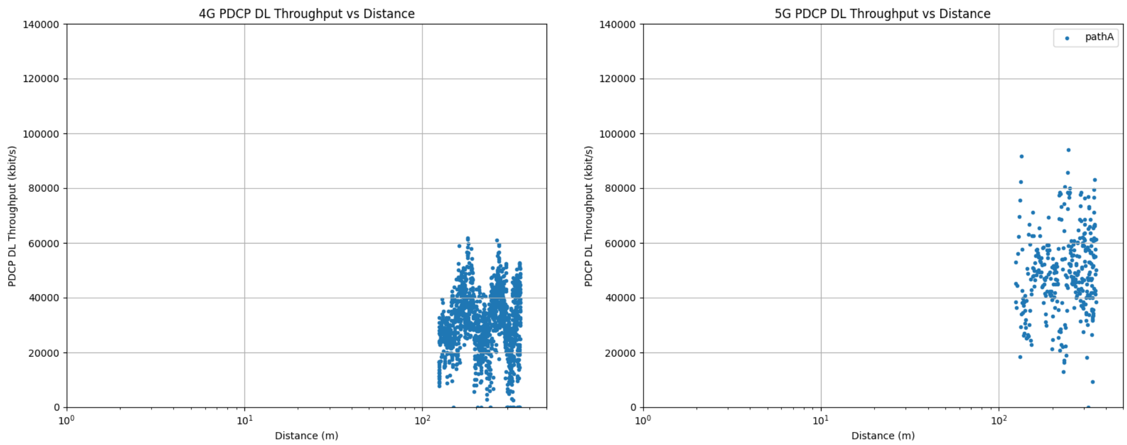

Figure A.15: Throughput versus distance for path A

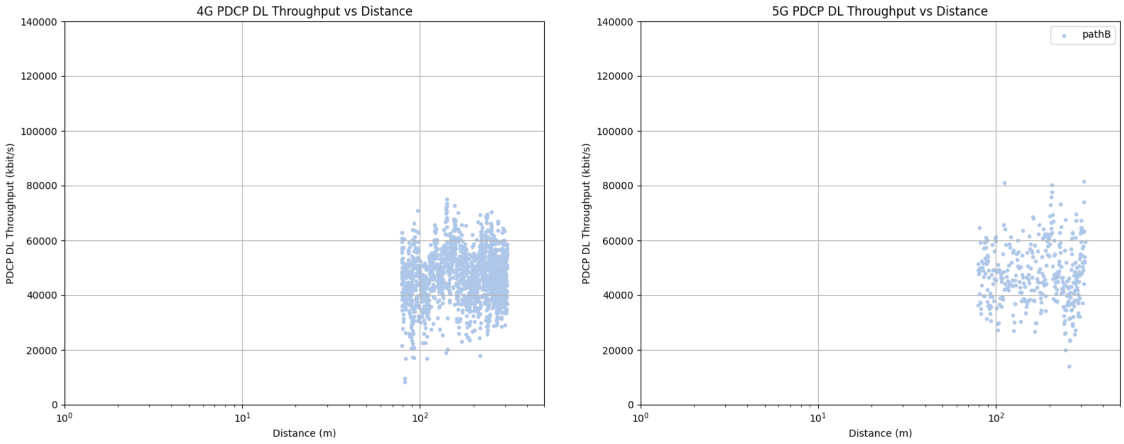

Figure A.16: Throughput versus distance for path B

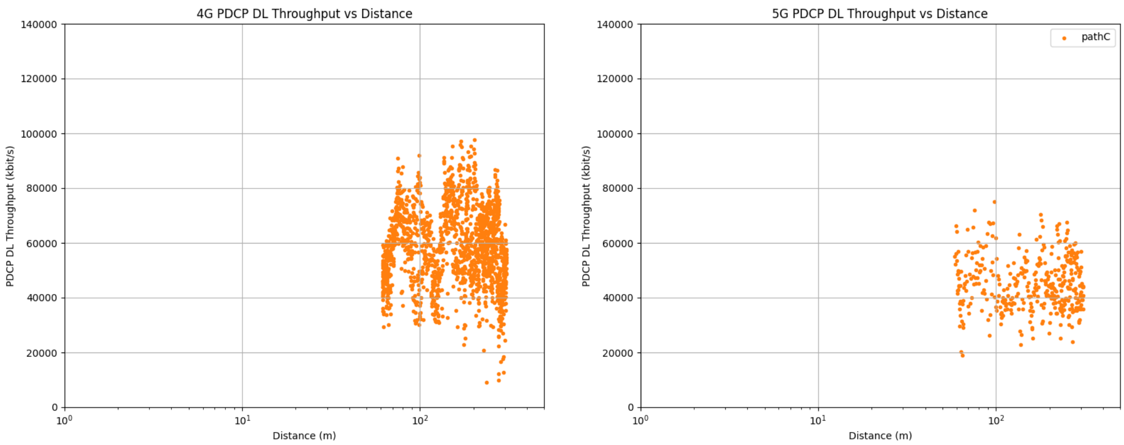

Figure A.17: Throughput versus distance for path C

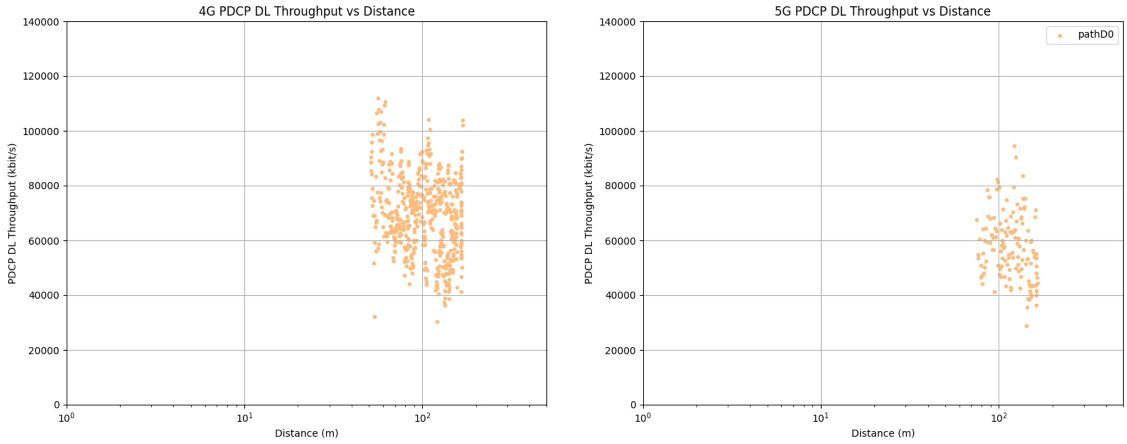

Figure A.18: Throughput versus distance for path D0

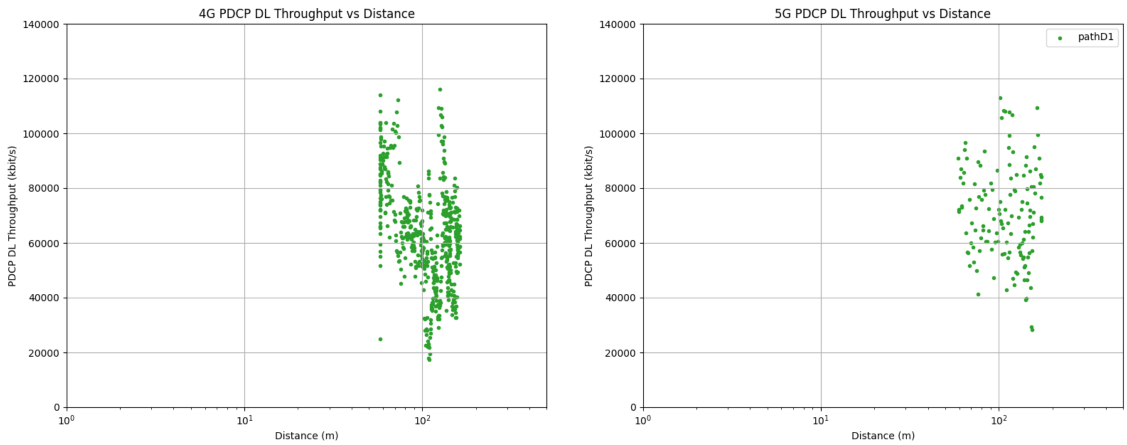

Figure A.19: Throughput versus distance for path D1

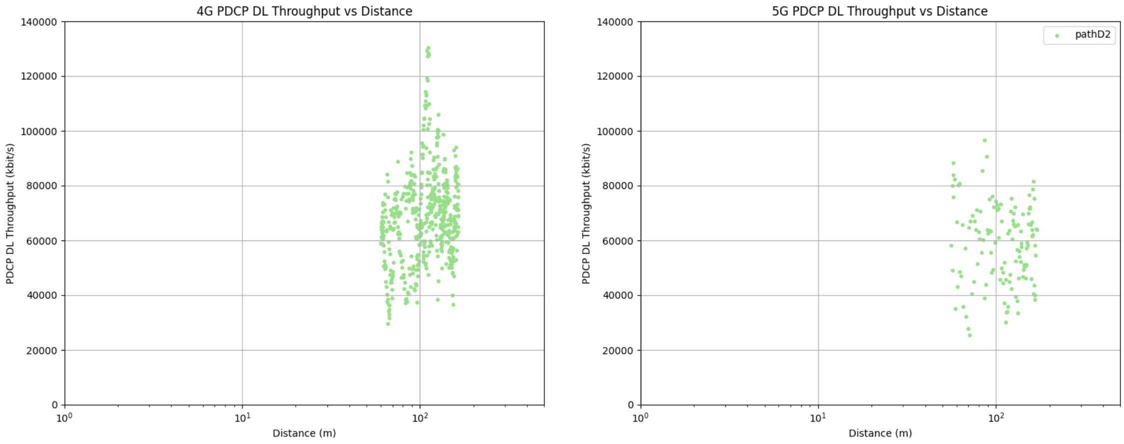

Figure A.20: Throughput versus distance for path D2

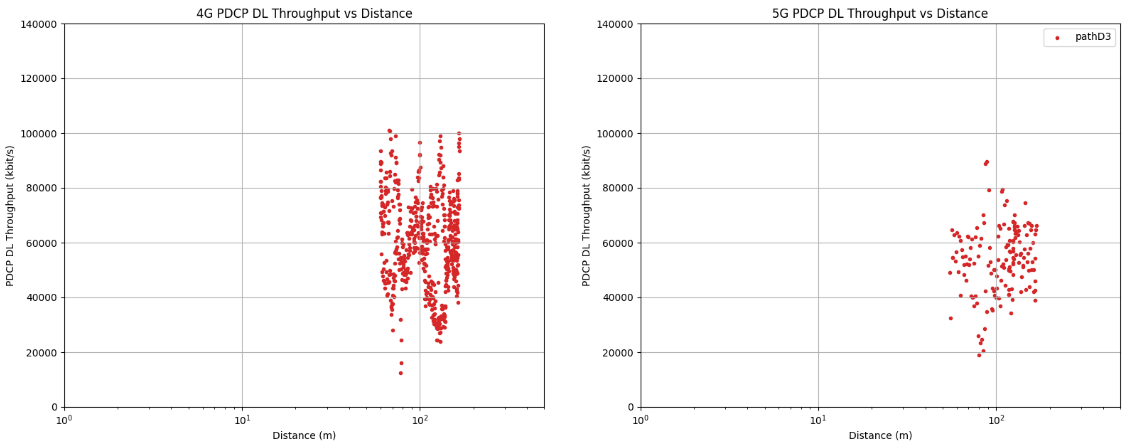

Figure A.21: Throughput versus distance for path D3

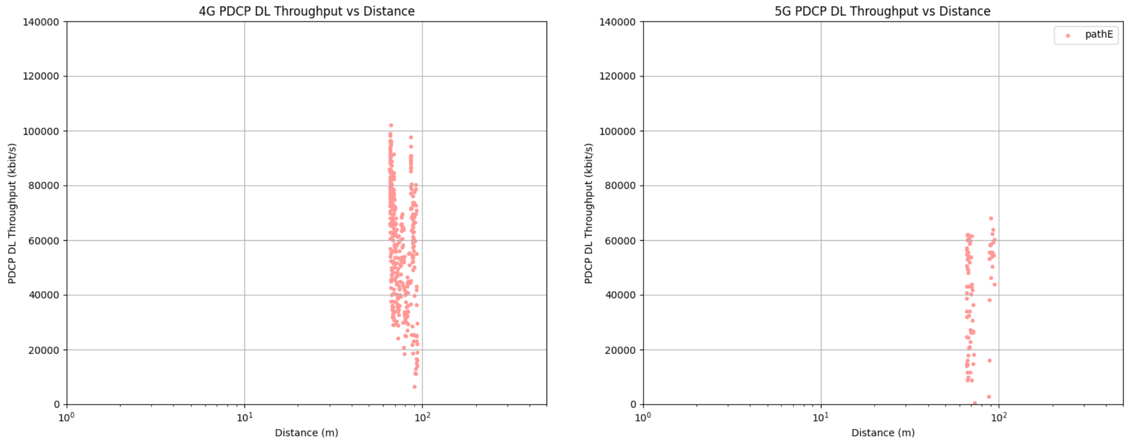

Figure A.22: Throughput versus distance for path E

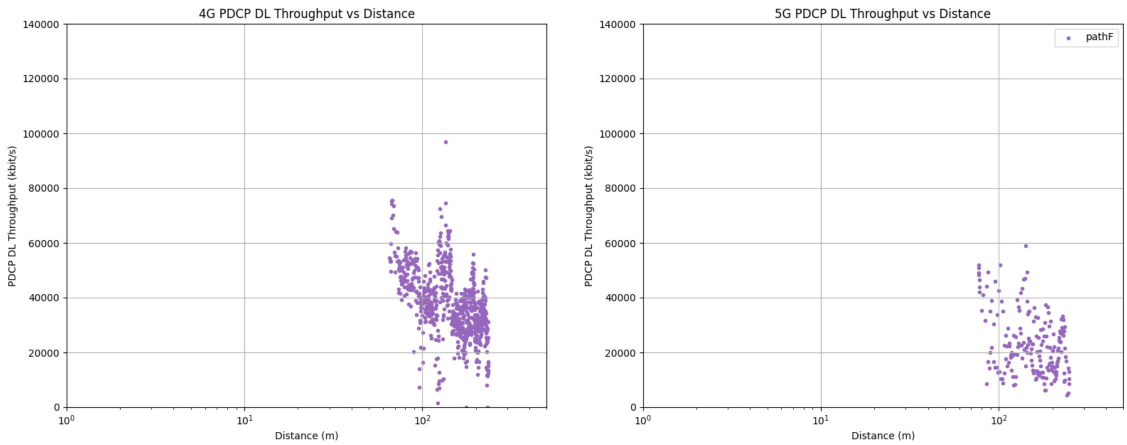

Figure A.23: Throughput versus distance for path F

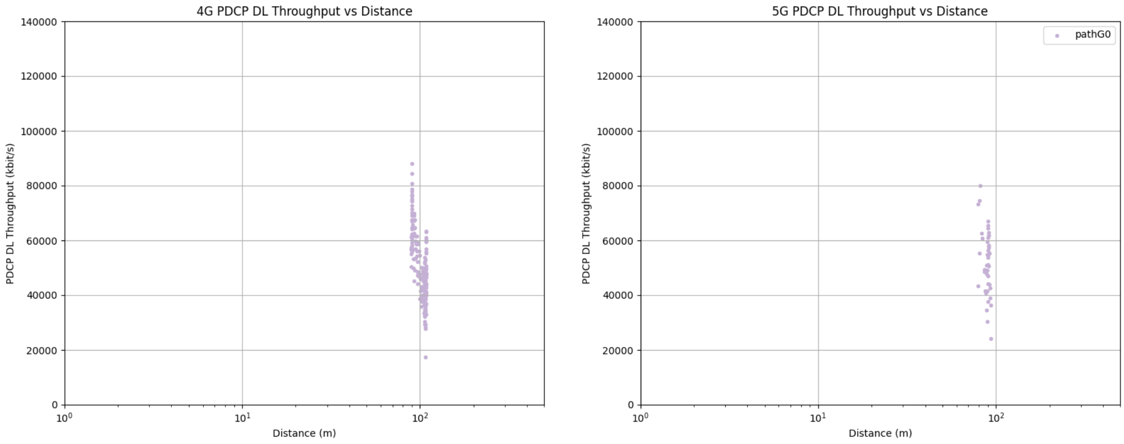

Figure A.24: Throughput versus distance for path G0

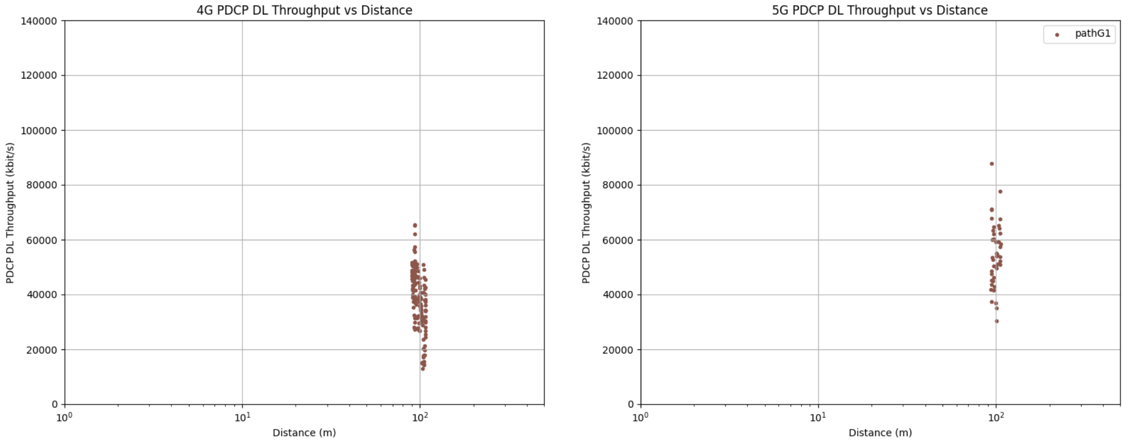

Figure A.25: Throughput versus distance for path G1

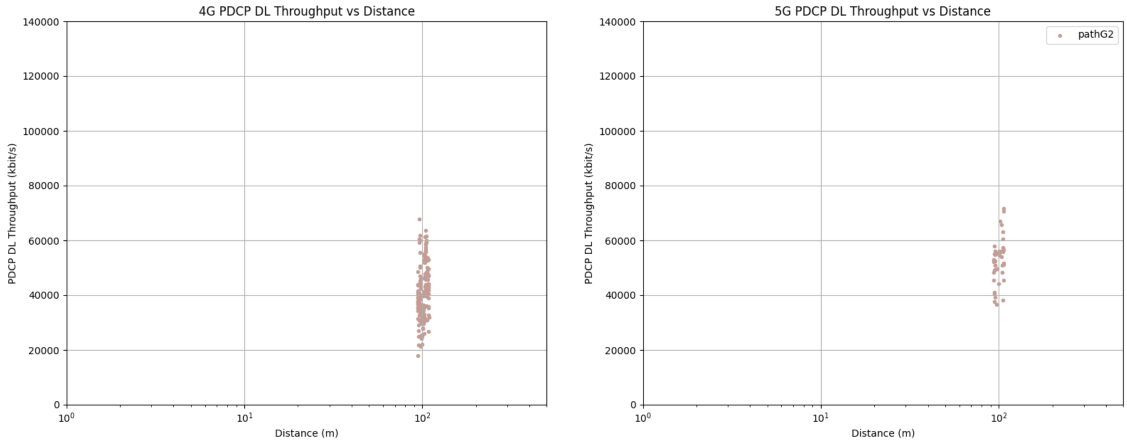

Figure A.26: Throughput versus distance for path G2

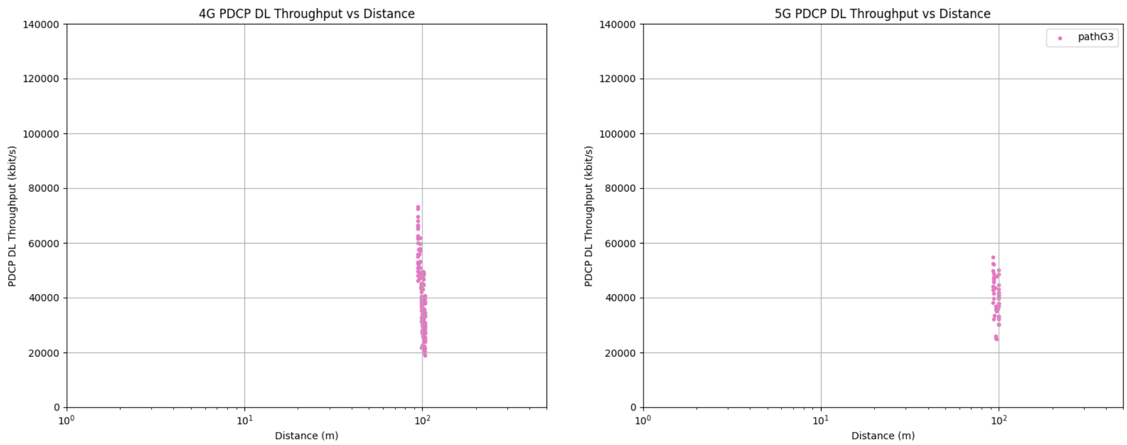

Figure A.27: Throughput versus distance for path G3

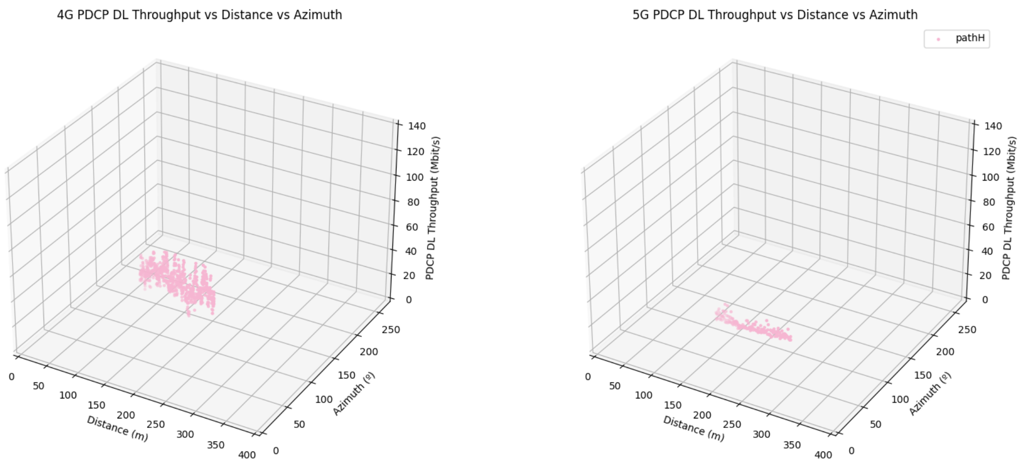

Figure A.28: Throughput versus distance versus azimuth for path H

A.3 Single plots for throughput versus distance versus azimuth

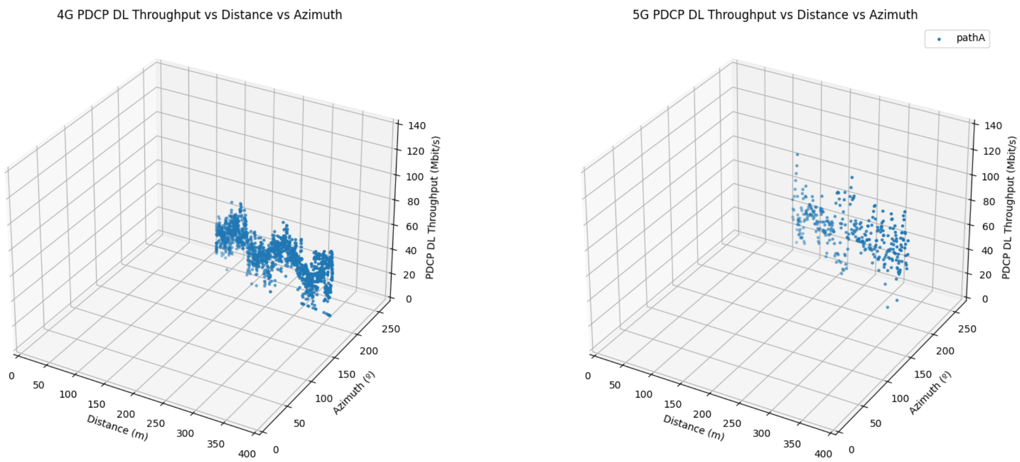

Figure A.29: Throughput versus distance versus azimuth for path A

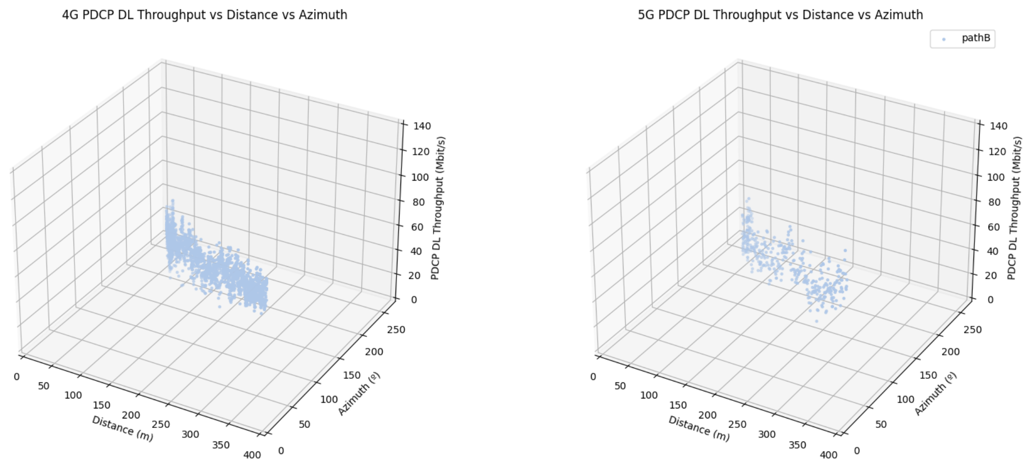

Figure A.30: Throughput versus distance versus azimuth for path B

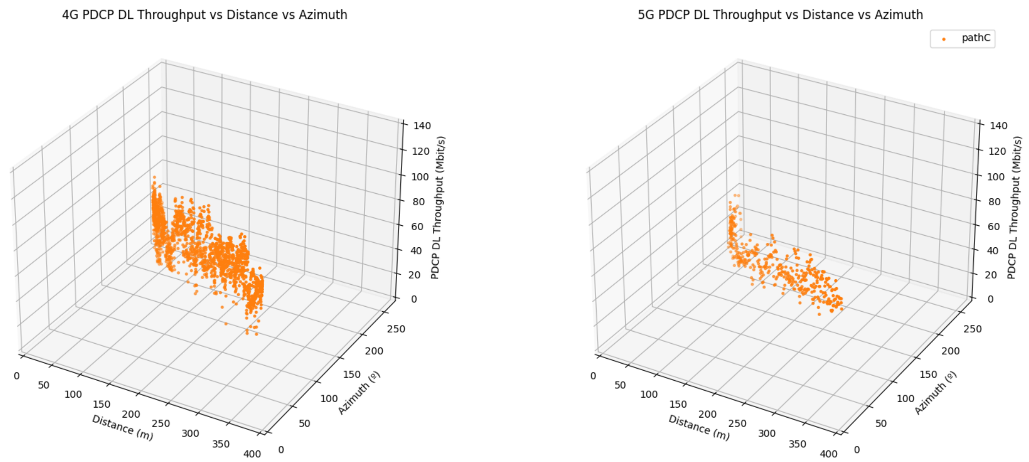

Figure A.31: Throughput versus distance versus azimuth for path C

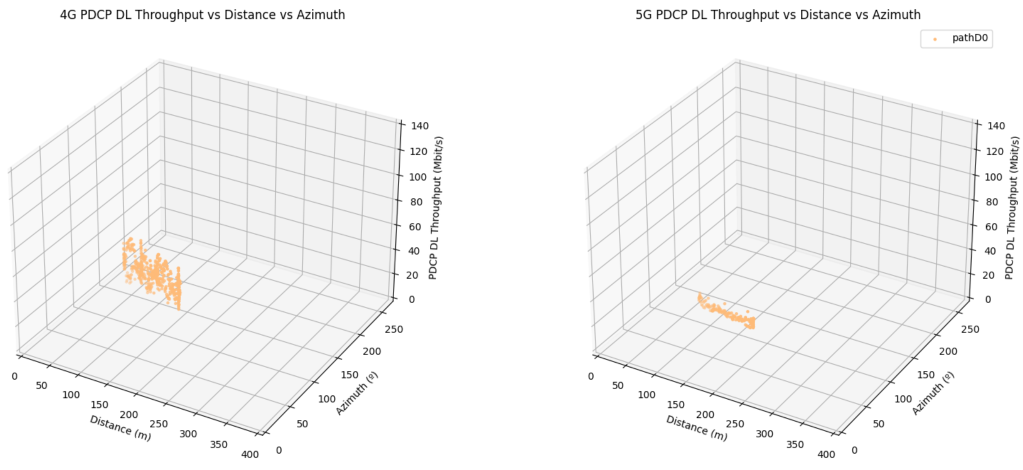

Figure A.32: Throughput versus distance versus azimuth for path D0

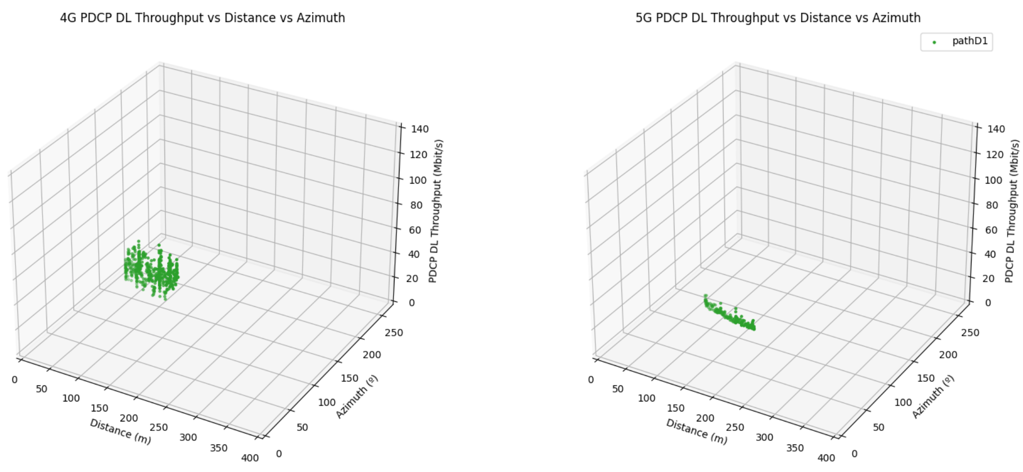

Figure A.33: Throughput versus distance versus azimuth for path D1

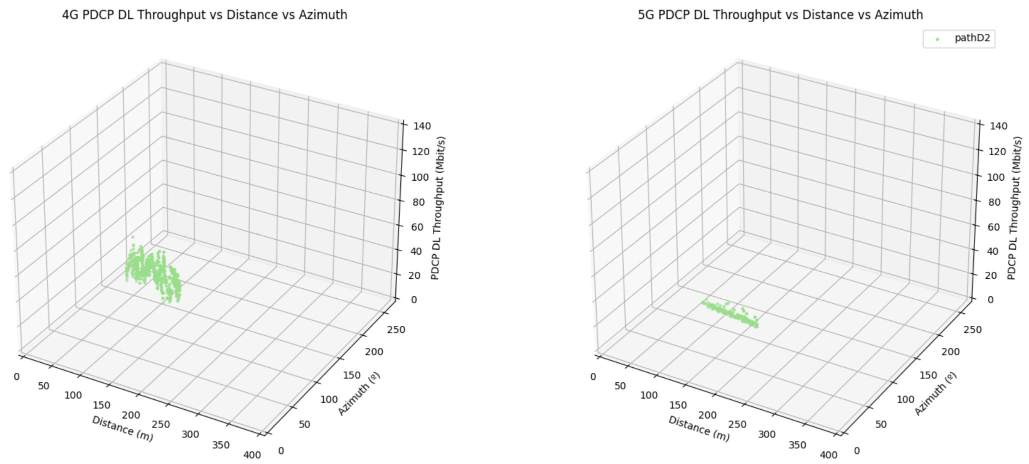

Figure A.34: Throughput versus distance versus azimuth for path D2

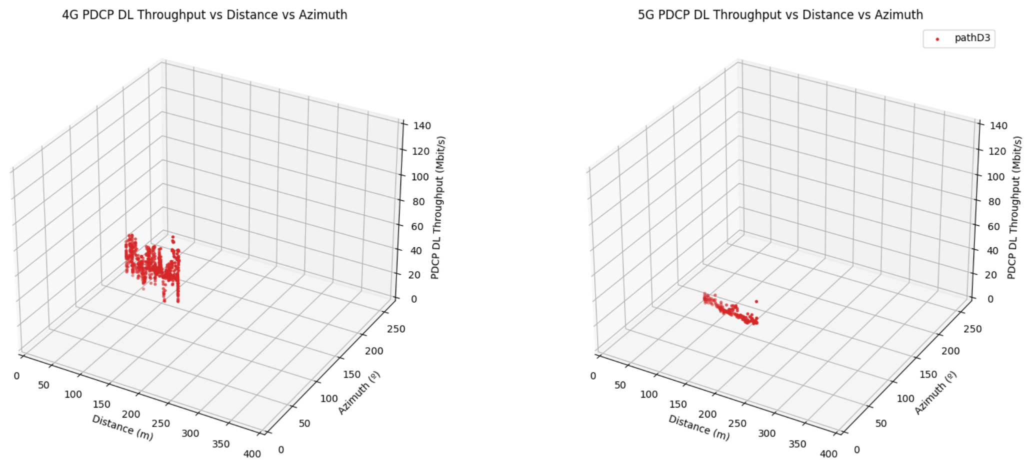

Figure A.35: Throughput versus distance versus azimuth for path D3

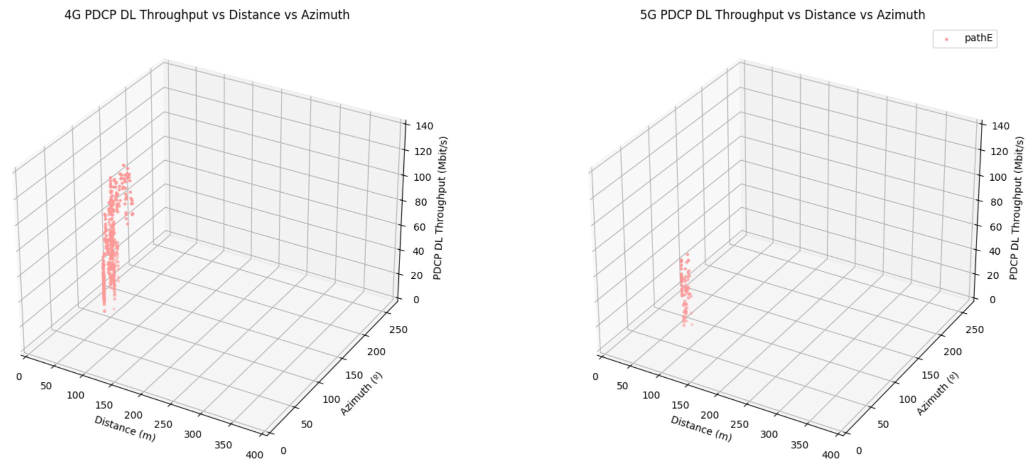

Figure A.36: Throughput versus distance versus azimuth for path E

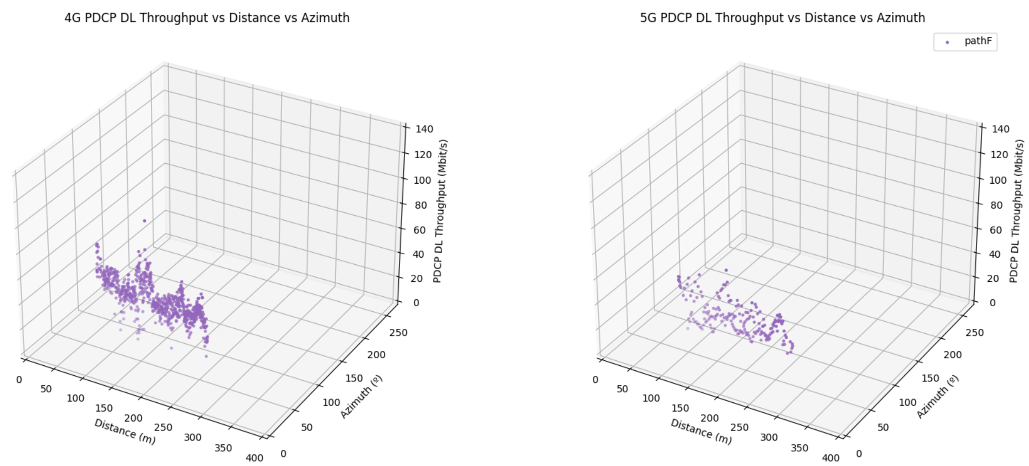

Figure A.37: Throughput versus distance versus azimuth for path F

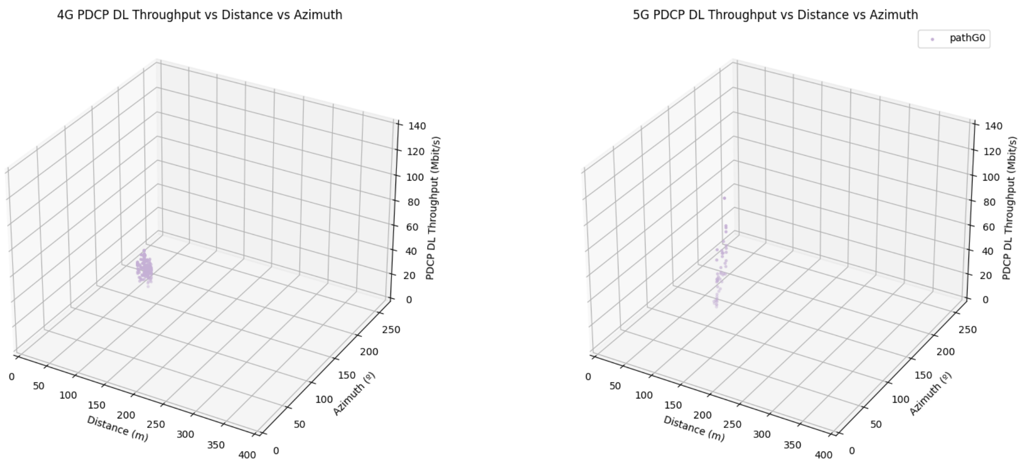

Figure A.38: Throughput versus distance versus azimuth for path G0

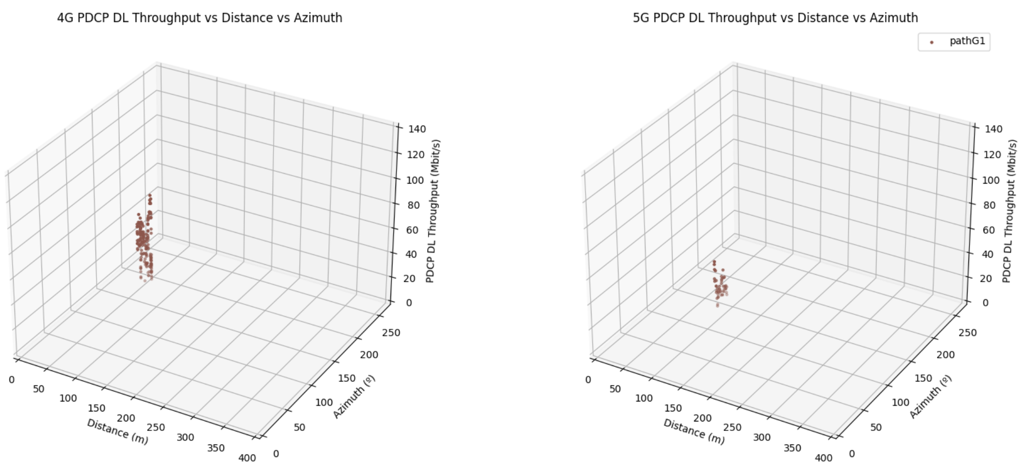

Figure A.39: Throughput versus distance versus azimuth for path G1

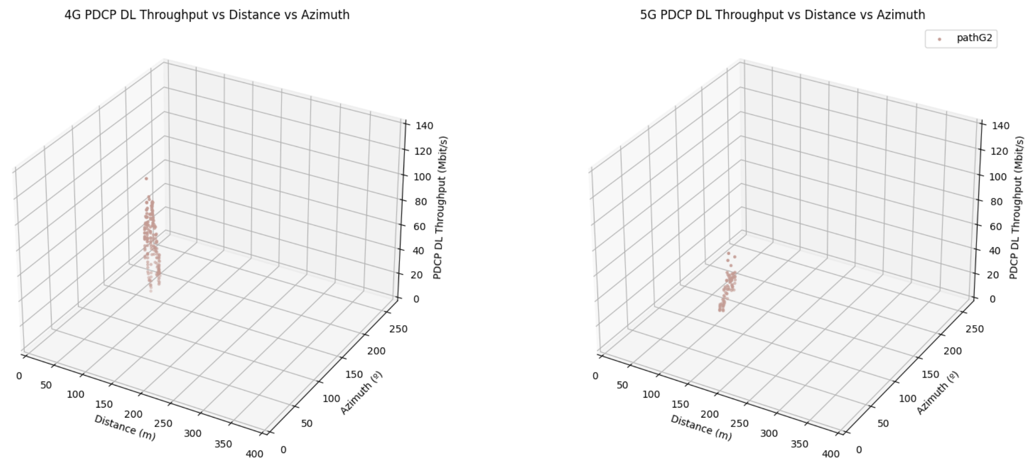

Figure A.40: Throughput versus distance versus azimuth for path G2

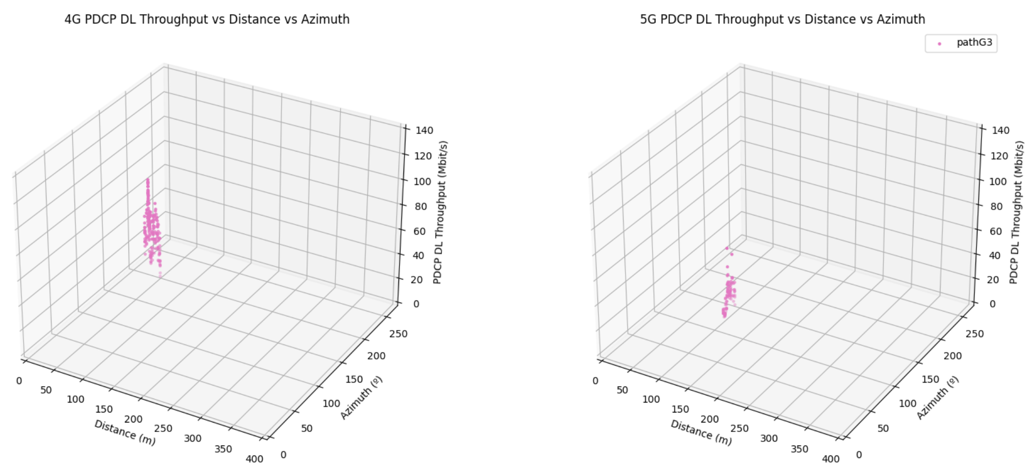

Figure A.41: Throughput versus distance versus azimuth for path G3

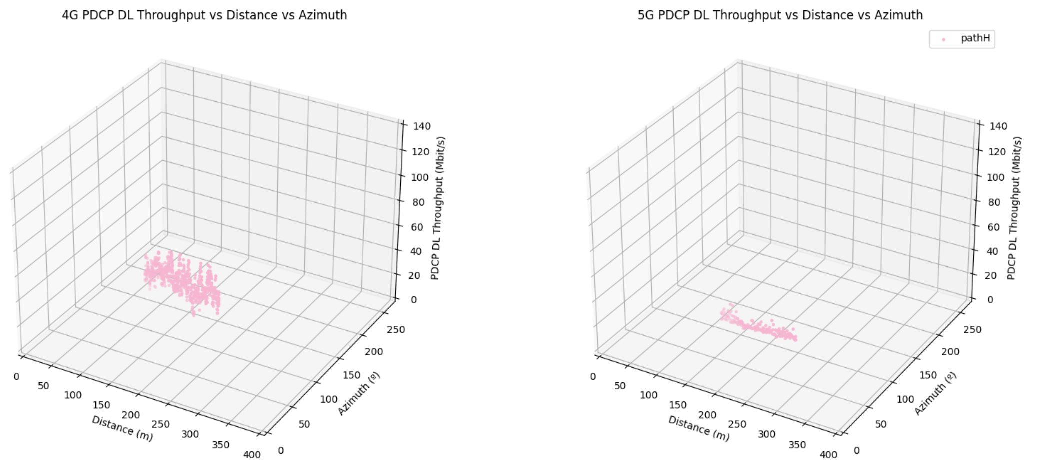

Figure A.42: Throughput versus distance versus azimuth for path H

References

[1] 5g architecture options. (2016, June). telecoms.com. Retrieved May 18, 2021, from https://telecoms.com/.

[2] 5g frequency bands in europe. (2020). https://www.everythingrf.com/. Retrieved July 10, 2021, from https://www.everythingrf.com/community/5g-frequency-bands-in-europe.

[3] 5g nr physical layer measurements (3gpp ts 38.215 version 15.2.0 release 15). (2020). https://www.etsi.org/. Retrieved July 10, 2021, from https://www.etsi.org/deliver/etsi_ts/138200_138299/138215/15.02.00_60/ts_138215v150200p.pdf.

[4] 5g sa versus 5g nsa: What's the difference? (2020). https://support.oppo.com/. Retrieved July 10, 2021, from https://support.oppo.com/ng/answer/?aid=neu11996.

[5] 5g spectrum bands explained. (2020). https://www.nokia.com/. Retrieved July 10, 2021, from https://www.nokia.com/networks/insights/spectrum-bands-5g-world/.

[6] 5g spectrum position. (2015). https://www.gsma.com. Retrieved May 13, 2021, from https://www.gsma.com/spectrum/wp-content/uploads/2021/04/5G-Spectrum-Positions.pdf.

[7] 5g spectrum position. (2008). https://www.nxp.com. Retrieved May 13, 2021, from https://www.nxp.com/docs/en/white-paper/LTEPTCLOVWWP.pdf.

[8] Etsi ts 136 314 v10.1.0 (2011-06)technical specificationlte;evolved universal terrestrial radio access (e-utra);layer 2 - measurements (3gpp ts 36.314 version 10.1.0 release 10). (2011, June). etsi.org. Retrieved May 18, 2021, from https://www.etsi.org.

[9] Industries' expectations for 5g. (2008). https://www.ericsson.com/. Retrieved October 25, 2020, from https://www.ericsson.com/490506/assets/local/mobility-report/documents/2019/emr-wef-industries-expectations.pdf.

[10] Lte;evolved universal terrestrial radio access (e-utra); physical layer; measurements (3gpp ts 36.214 version 14.2.0 release 14)). (2017, April). etsi.org. Retrieved May 18, 2021, from https://www.etsi.org/deliver/etsi_ts/136200_136299/136214/14.02.00_60/ts_136214v140200p.pdf.

[11] Making 5g nr a reality. (2008). https://www.qualcomm.com. Retrieved January 8, 2021, from https://www.qualcomm.com/media/documents/files/whitepaper-making-5g-nr-a-reality.pdf.

[12] New radio. (2020). https://www.ni.com/. Retrieved July 10, 2021, from https://www.ni.com/pt-pt/innovations/wireless/5g/new-radio.html.

[13] Tems pocket user's manual. (2015). http://www.adinstruments.es. Retrieved April 22, 2021, from http://www.adinstruments.es/WebRoot/StoreLES/Shops/62688782/5B63/5797/3B43/DD36/DD66/0A0C/6D09/0C3F/TEMS-Pocket-15-1-User-Manual.pdf.

[14] Mamta Agiwal, Abhishek Roy, and Navrati Saxena. Next generation 5g wireless networks: A comprehensive survey. *IEEE Communications Surveys Tutorials*, 18(3):1617–1655, 2016.

[15] Erik Dahlman, Gunnar Mildh, Stefan Parkvall, Janne Peisa, Joachim Sachs, Yngve Selén, and Johan Sköld. 5g wireless access: requirements and realization. *IEEE Communications Magazine*, 52(12):42–47, 2014.

[16] Andrea Goldsmith. *Wireless Communications*. Cambridge University Press, 2005.

[17] A. Gupta and R. K. Jha. A survey of 5g network: Architecture and emerging technologies. *IEEE Access*, 3:1206–1232, 2015.

[18] Charles R. Harris, K. Jarrod Millman, Stéfan J. van der Walt, Ralf Gommers, Pauli Virtanen, David Cournapeau, Eric Wieser, Julian Taylor, Sebastian Berg, Nathaniel J. Smith, Robert Kern, Matti Picus, Stephan Hoyer, Marten H. van Kerkwijk, Matthew Brett, Allan Haldane, Jaime Fernández del Río, Mark Wiebe, Pearu Peterson, Pierre Gérard-Marchant, Kevin Sheppard, Tyler Reddy, Warren Weckesser, Hameer Abbasi, Christoph Gohlke, and Travis E. Oliphant. Array programming with NumPy. *Nature*, 585(7825):357–362, September 2020.

[19] J. D. Hunter. Matplotlib: A 2d graphics environment. *Computing in Science & Engineering*, 9(3):90–95, 2007.

[20] Meik Kottkamp, Anil Pandey, Andreas Roessler, Reiner Stuhlfauth, and Daniela Raddino. *5G New Radio - Fundamentals, Procedures, Testing Aspects*. Rohde Schwarz GmbH KG, Second edition, 2019.

[21] Anurag Kumar, D. Manjunath, and Joy Kuri. *Wireless Networking*. Morgan Kaufmann Publishers Inc., San Francisco, CA, USA, 2008.

[22] Andrea Lopes, I. Batalha, and Cristiane Gomes. Large-scale analysis and modeling for indoor propagation at 10 ghz. *Journal of Microwaves, Optoelectronics and Electromagnetic Applications*, 19:276–293, 06 2020.

[23] Lu Lu, Geoffrey Ye Li, A. Lee Swindlehurst, Alexei Ashikhmin, and Rui Zhang. An overview of massive mimo: Benefits and challenges. *IEEE Journal of Selected Topics in Signal Processing*, 8(5):742–758, 2014.

[24] The pandas development team. pandas-dev/pandas: Pandas, February 2020.

[25] Giulia Sanfilippo, Olga Galinina, Sergey Andreev, Sara Pizzi, and Giuseppe Araniti. A concise review of 5g new radio capabilities for directional access at mmwave frequencies, 2018.

[26] M. Simsek, A. Aijaz, M. Dohler, J. Sachs, and G. Fettweis. 5g-enabled tactile internet. *IEEE Journal on Selected Areas in Communications*, 34(3):460–473, 2016.

[27] Erik G. Ström, Petar Popovski, and Joachim Sachs. 5g ultra-reliable vehicular communication. *CoRR*, abs/1510.01288, 2015.

[28] Shu Sun, Theodore S. Rappaport, Sundeep Rangan, Timothy A. Thomas, Amitava Ghosh, Istvan Z. Kovacs, Ignacio Rodriguez, Ozge Koymen, Andrzej Partyka, and Jan Jarvelainen. Propagation path loss models for 5g urban micro- and macro-cellular scenarios. In *2016 IEEE 83rd Vehicular Technology Conference (VTC Spring)*, pages 1–6, 2016.

[29] Timothy A. Thomas, Marcin Rybakowski, Shu Sun, Theodore S. Rappaport, Huan Nguyen, Istvan Z. Kovacs, and Ignacio Rodriguez. A prediction study of path loss models from 2-73.5 ghz in an urban-macro environment. In *2016 IEEE 83rd Vehicular Technology Conference (VTC Spring)*, pages 1–5, 2016.

[30] Takuya Tojo, Hiroki Baba, Seisho Yasukawa, and Yoshikatsu Okazaki. Micro-burst analysis and mitigation for 5g low-latency communication services. In *2019 IEEE 2nd 5G World Forum (5GWF)*, pages 232–236, 2019.

[31] Guido Van Rossum. *The Python Library Reference, release 3.8.2*. Python Software Foundation, 2020.

[32] Frederick W. Vook, Amitava Ghosh, and Timothy A. Thomas. Mimo and beamforming solutions for 5g technology. In *2014 IEEE MTT-S International Microwave Symposium (IMS2014)*, pages 1–4, 2014.

[33] Dongzhu Xu, Anfu Zhou, Xinyu Zhang, Guixian Wang, Xi Liu, Congkai An, Yiming Shi, Liang Liu, and Huadong Ma. Understanding operational 5g: A first measurement study on its coverage, performance and energy consumption. page 479–494, 2020.